



OPEN ACCESS

EDITED BY

Wei Ju,
China University of Mining and
Technology, China

REVIEWED BY

Jin Lai,
China University of Petroleum, China
Hongwei Yin,
Nanjing University, China

*CORRESPONDENCE

Ziqi Zhong,
✉ 2101110667@pku.edu.cn

SPECIALTY SECTION

This article was submitted to Structural
Geology and Tectonics,
a section of the journal
Frontiers in Earth Science

RECEIVED 17 November 2022

ACCEPTED 23 January 2023

PUBLISHED 03 February 2023

CITATION

Zhong Z, Xia J, Huang S, Luo C, Chang H,
Li X, Wei L and Zhang H (2023),
Reconstruction of proto-type basin and
tectono-paleogeography of Tarim block in
early Paleozoic.
Front. Earth Sci. 11:1101360.
doi: 10.3389/feart.2023.1101360

COPYRIGHT

© 2023 Zhong, Xia, Huang, Luo, Chang, Li,
Wei and Zhang. This is an open-access
article distributed under the terms of the
[Creative Commons Attribution License
\(CC BY\)](https://creativecommons.org/licenses/by/4.0/). The use, distribution or
reproduction in other forums is permitted,
provided the original author(s) and the
copyright owner(s) are credited and that
the original publication in this journal is
cited, in accordance with accepted
academic practice. No use, distribution or
reproduction is permitted which does not
comply with these terms.

Reconstruction of proto-type basin and tectono-paleogeography of Tarim block in early Paleozoic

Ziqi Zhong^{1*}, Jinkai Xia¹, Shaoying Huang², Caiming Luo²,
Haining Chang¹, Xiang Li¹, Lunyan Wei¹ and Hao Zhang¹

¹The Key Laboratory of Orogenic Belts and Crustal Evolution, Ministry of Education, School of Earth and Space Sciences, Peking University, Beijing, China, ²Institute of Petroleum Exploration and Development, Tarim Oilfield Company, Korla, China

Tarim Basin is a large, superimposed basin rich in petroleum resources, which has experienced many stages of complex tectonic-sedimentary evolution. As the basic geological study of the Tarim Basin, the proto-type basin and tectono-paleogeographic evolution are of great significance for understanding the distribution of petroleum reservoirs in the superimposed basin and provide tectonic background and theoretical guidance for petroleum exploration. According to the residual thickness map, as well as other lithofacies and seismic data, the scopes of the proto-type basin are determined by the marginal facies method and the thickness trend method, and the shortening amounts are calculated by the balanced cross-section method. Based on these data and previous works, four proto-type basin maps of Tarim Basin in present-day geographic coordinates and four tectono-paleogeographic maps of Tarim Basin in paleogeographic coordinates during the early Paleozoic are reconstructed, which directly show the changes of sedimentary and uplift-depression pattern caused by the transformation of the tectonic environment from extension to compression. In the Cambrian, the Tarim Basin was controlled by the extensional tectonic environment, with the sedimentary framework of "carbonate platform in the west, deep-water basin in the east". At the end of the Ordovician, the Kudi Ocean and the North Altyn Ocean were closed, and the Central and South Kunlun terrane and the Altyn-Qilian terrane were collaged with the Tarim block, which directly led to the transformation of the uplift-depression pattern in the Tarim Basin from east-west differentiation to north-south differentiation, thus changing the sedimentary environment of the Tarim Basin in the late Ordovician to Silurian.

KEYWORDS

Tarim basin, early paleozoic, proto-type basin, tectono-paleogeography, evolution

1 Introduction

Tarim Basin is a large, superimposed basin in northwest China, located between the Qinghai-Tibet Plateau and Tianshan Mountains, covering an area of more than 560,000 square kilometers. It has great potential for petroleum exploration (Li et al., 2019; Tian et al., 2021), and its rich petroleum resources depend on good reservoir-forming conditions, which means that the exploration of petroleum resources needs sufficient basic geological research as a support. The Tarim Basin developed on the Tarim block and underwent multiple stages of complex tectonic-sedimentary evolution (Jia., 1997; He et al., 2005; Lin et al., 2011; Li et al., 2015). The evolutionary history of the Tarim block involves the convergence and disintegration of several supercontinents, including the Rodinia and the Gondwana supercontinent (Xu et al., 2011; Torsvik and Cocks, 2013; Li et al., 2014, 2015; Maruyama et al., 2014; He et al., 2015).

Many achievements have been made in the study of the Tarim proto-type basin and tectono-paleogeography in the early Paleozoic (Chen et al., 2015; Gao et al., 2016, 2017a, 2017b; Tian et al., 2018), but there is a lack of research on the systematic combination of the tectonic background and the proto-type basin. The Tarim Basin has experienced many stages of complex tectonic evolution and the superimposed geological evolution of multiple original basins, which strongly reshaped the original paleogeographic features of the Tarim Basin. The peripheral background of each stage of the Tarim Basin is an intuitive reflection of tectonism, which is closely related to the restoration of the Tarim proto-type basin (Lin et al., 2011; Li et al., 2015; Wu et al., 2020). According to residual thickness maps, rock facies, drilling data, and numerous seismic profiles, the proto-type basin and tectono-paleogeographic maps of Tarim Basin in the early Paleozoic are reconstructed in the paper.

2 Geological setting and plate tectonic configuration

2.1 Regional setting

The Tarim block is located between the Central Asian orogenic belt and the Tethys domain, sandwiched between the West Kunlun, Altyn Tagh, and South Tianshan Mountains (Figure 1A). The Yili terrane, the Central Tianshan terrane, the Altyn-Qilian terrane, and the Central and South Kunlun terrane are distributed clockwise in the periphery of the Tarim block from south to north, bounded by the South Tianshan Ocean, North Altyn Ocean and Kudi Ocean in the early Paleozoic (Figure 1B). The Tarim Basin is composed of Archean-early Neoproterozoic metamorphic crystalline basement and thick Nanhua-Quaternary sedimentary rock series, which can be divided vertically into five structural layers: pre-Nanhua basement, Nanhua-Sinian rift basin, Cambrian-Ordovician marine carbonate platform, Silurian-Cretaceous clastic rock depression and Cenozoic foreland basin (Figure 1C, Jia., 2004; Lin et al., 2011; Wu et al., 2020; Wu et al., 2021). According to the unconformities, the sedimentary tectonic evolution of the Tarim Basin is divided into four major development and evolution stages, with seven tectonic episodes (Lin et al., 2011; Wu et al., 2020; Wu et al., 2021). The Sinian-late Devonian is the first stage, which is controlled by Caledonian movement and experiences a complete tectonic cycle (Figure 1C, Lin et al., 2008, 2011). In the early Paleozoic, the Tarim Basin was essentially in the marine environment and developed extensive marine deposits. During the Sinian to Silurian period, the oceans around the Tarim Basin experienced a process of expansion to closure, which played a decisive role in the internal subsidence and filling evolution model of the basin.

In the late Proterozoic to early Cambrian, the Tarim Basin was in the stage of rapid extensional subsidence, accompanied by the development of a series of rifts (Xu et al., 2008; Yun et al., 2014; Wu et al., 2016; Wu et al., 2018; Wu et al., 2020; Wang T et al., 2021), with the pattern of “uplift in the south and depression in the north”. In the Cambrian to early Ordovician, the Tarim block has been separated from the Rodinia supercontinent (Figure 1C), located on the north shore of the original Tethys Ocean (Li et al., 2008; Li et al., 2010; Dong et al., 2018), developing a large carbonate platform with a thickness of more than 2000 m (Li et al., 2010; Gao and Fan, 2015; Gao et al., 2017a). At the end of the early Ordovician, the South Paleo-Tethys

Ocean began to subduct (Li et al., 2017; Dong et al., 2018), forming the E-W trending paleo-uplift in the basin by the compression from the south, which was finalized at the end of the Ordovician (Wu et al., 2016). In the late Ordovician, with the closure of the Kudi Ocean and the North Altyn Ocean (Figure 1C, Jia., 2004; Li et al., 2017), the Tarim Basin underwent a great transition from extension to extrusion, and a large area of uplift and denudation occurred in the south and east of the basin, forming a widely distributed unconformity. This situation became more and more intense in the late Ordovician, and the north-south differentiation pattern was formed (Gao et al., 2012; Gao et al., 2016; Gao et al., 2017b; Wu et al., 2016). During the Silurian, the southern part of the Tarim Basin was uplifted on a large scale, and deposits were only developed in the north of the Central Uplift Belt (Figure 1C, Lin et al., 2011, 2012; Zheng et al., 2014).

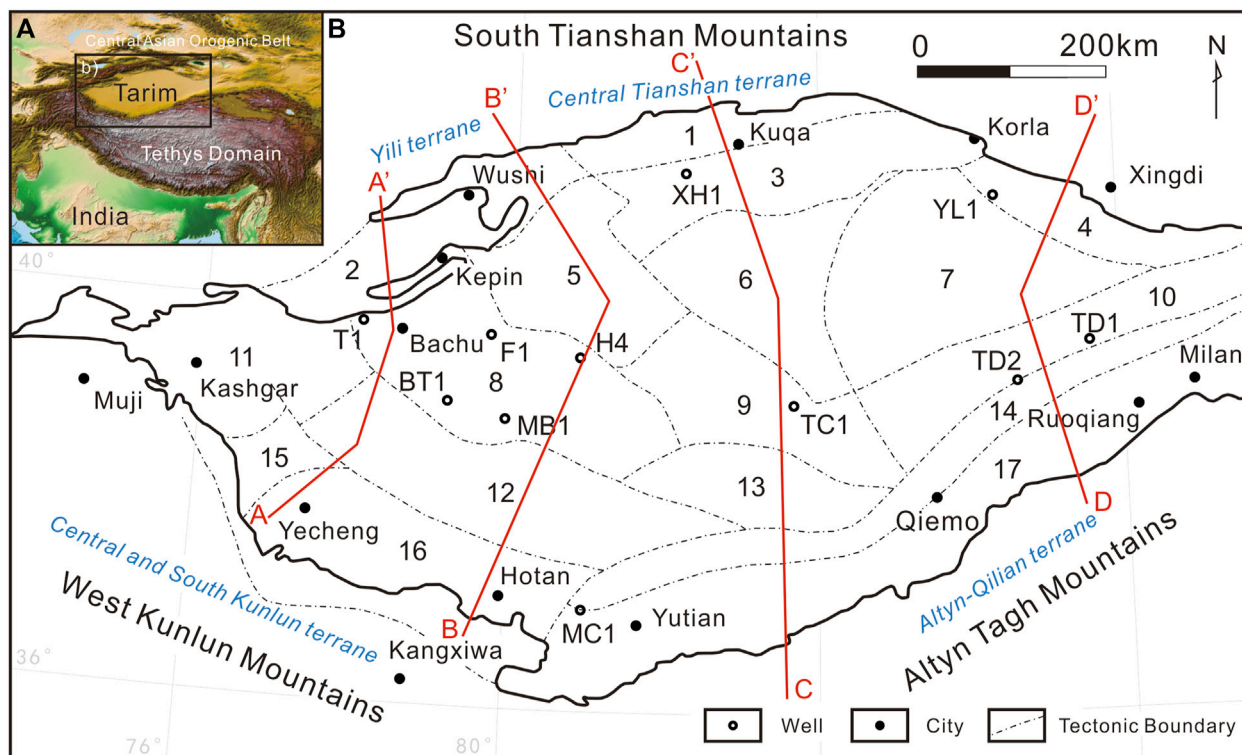
2.2 Tarim block in the global plate tectonics and its evolution

Restoring the position of paleo-continent or block in deep time is an important part in the paleogeographic reconstruction, and paleomagnetism is the only quantitative tool. By reconstructing the paleomagnetic field, the paleo-latitude, direction, and rotation of the block can be obtained (Torsvik and Cocks, 2004; Hou et al., 2008; Hou et al., 2020; Torsvik et al., 2016; Torsvik and Cocks, 2019). However, the paleo-longitude position of the block cannot be determined by paleomagnetism, and the frequent reversal of paleomagnetism makes it impossible to determine whether the calculated paleolatitude is south latitude or north latitude. At this point, other geological evidence, such as paleontology (Cocks and Torsvik, 2002; Cao et al., 2017), sediment facies, orogenic belts, magmatic activity (Steinberger et al., 2004; Torsvik et al., 2016), marine geophysics (Matthews et al., 2016), and so on, are needed.

- (1) The paleogeographic location of the Tarim block based on paleomagnetism

For the Tarim block, on the one hand, due to the large-scale magmatic activity in the Paleo-Asian Oceanic tectonic domain at the end of the late Paleozoic (Xiao et al., 2009) and the significant tectonic deformation caused by the collision between India and the Asian continent in the Cenozoic (Johnson., 2002; Huang et al., 2009), most of the magnetic materials in the early Paleozoic experienced heavy magnetization and could not effectively record the paleogeographic location at that time. On the other hand, the early Paleozoic strata in Tarim Basin are mainly marine limestone and marl with weak magnetism, so it is difficult to obtain reliable primary remanence which represents the information of paleomagnetic field in the period of rock formation. So far, the reliable paleomagnetic data accumulated in the early Paleozoic era are very limited.

After Fischer statistics of these paleomagnetic poles with high confidence (Van der Voo., 1990), the paleomagnetic pole positions of the Tarim block in the early Paleozoic are obtained (Table 1, Li et al., 1990; Fang et al., 1996; Huang et al., 2019). Combined with the Apparent Polar Wander Paths (Wen et al., 2017) and peripheral geological background analysis, the global plate tectonic patterns are reconstructed in different periods of the early Paleozoic (Figure 2, late Cambrian, late Ordovician, and late Silurian).



Strata		Age (Ma)	Southeast Faulted-uplift	Tangguzibas Depression	Tazhong Uplift	Mangar Depression	Tabei Uplift	Basin Evolution	Tectonic Setting	
Devonian	D ₁₋₂	410	Intracratonic depression				Unconformity	Back-arc foreland basin	Closure of the Kudi Ocean and North Altny Ocean	
Silurian	S	440	Intracratonic depression basin				Uplift	Intracratonic depression basin		
Ordovician	O ₃	480	Back-arc foreland	Carbonate platform	Deep-water	Carbonate platform	Uplift	Back-arc foreland basin	Cratonic platform	
	O ₁₋₂		Intracratonic platform				Uplift	Intracratonic platform		
Cambrian	Є ₃	540	Restricted platform				Deep-water	Carbonate platform	Passive continental margin	Breakup of the Rodinia Supercontinent
	Є ₂		Carbonate platform				Deep-water	Carbonate platform	Passive continental margin	
	Є ₁		Carbonate platform				Deep-water	Carbonate platform	Passive continental margin	
Sinian	Z	630	Carbonate platform				Rift-aulacogen	Passive continental margin	Formation of the Rodinia Supercontinent	
Nanhua	Nh	735	Rift-aulacogen				Rift-aulacogen	Crystalline basement		
Lower-Middle Proterozoic	Pt ₁₋₂		Limestone	Dolomite	Mudstone	Conglomerate	Sandstone	Igneous rock		

FIGURE 1

(A) Location of the Tarim Basin. (B) Tectonic framework of the Tarim Basin (modified after He et al., 2016). Structural units of the Tarim Basin: 1-Kuqa Depression; 2-Kepingtage Faulted-uplift; 3-Tabei Uplift; 4-Kongquehe Slope; 5-Awati Depression; 6-Shuntuoquole Uplift; 7-Manjiaer Depression; 8-Bachu Uplift; 9-Tazhong Uplift; 10-Guchengxu Uplift; 11-Kashi Depression; 12-Maigaiti Slope; 13-Tangguzibas Depression; 14-Tanan Uplift; 15-Shache Bulge; 16-Yecheng Depression; 17-Southeast Depression. The shortening amount is integrated on four representative lines (AA', BB', CC' and DD' in Table 2), which are red lines. (C) Tectonic-sedimentary evolution sequence of Tarim Basin in the middle-late Proterozoic to Devonian (modified after Lin et al., 2011).

The Tarim block was located in the middle-low latitude of the southern Hemisphere during the late Cambrian period (Table 1, Figure 2A, Huang et al., 2018; Zhao et al., 2018), along with the South China block on the western side of the Gondwana supercontinent. The periphery of the Tarim block is in a passive

continental margin environment, and although the original Tethys Ocean has been formed between the Tarim block and Australia plate, they are still related and similar in many aspects (Figure 2A, Zhao et al., 2018). At this time, the eastern continental groups, such as North China block and Siberia plate, have shifted from the other side of the

TABLE 1 Summary of available Early Paleozoic paleomagnetic poles for the Tarim block. Slat = Sampling locality Latitude; SLong = Sampling locality Longitude; N/n = Number of sites/number of samples; Plat = Pole Latitude; Plong = Pole Longitude; A₉₅ = 95% confidence oval (or dp/dm, semi minor and major axes of 95% confidence ellipsoid). Cam, O, S, and D indicate the Cambrian, Ordovician, Silurian, and Devonian times with 1= Early, 2 = Middle, and 3 = Late.

Age	Lithology	Locality	Slat	Slong	N/n	Plat	Plong	A ₉₅	Reference
S ₃ -D ₂	Sandstones	Kalpin	40.5	78.8	3/-	9.8	152.7	3.6/5.5	Fang et al., 1996
S ₁ -D ₂	Limestones	Tarim	40.6	79.0	-/40	16.5	165.2	2.9/5.3	Li et al., 1990
S ₂	Sandstones	Kalpin	40.6	79.6	4/-	12.1	158.4	4.1/7.2	Fang et al., 1996
S ₁₋₂	Sandstones	Kalpin	40.5	78.7	10/70	19.1	172.9	5.5	Huang et al., 2019
O ₂₋₃	Limestones	Kalpin and Aksu	40.6	78.9	-/99	-33.5	185.3	2.8/4.1	Huang et al., 2019
O ₁	Limestones	Yaerdang Mountains	41.3	83.4	3/-	-20.4	180.6	8.5/15	Fang et al., 1996
Cam ₂ -O ₂	Limestones	Yaerdang Mountains	41.3	83.4	5/15	-46.1	188.9	6.1/8.8	Sinopec Research Report

earth to the Western Hemisphere (Huang et al., 2018), and the three Chinese blocks (North China block, South China block, and Tarim block) show an N-S/T pattern (Figure 2A, Zhao et al., 2018).

After the middle-late Ordovician, the close relationship between the South China block and the Gondwana supercontinent is likely to last until the middle Devonian (Yang et al., 2004), while the Tarim block, located on the outermost margin of the Gondwana supercontinent, separated from it with its rapid clockwise rotation (Van der Voo, 1993) and moved northwestward rapidly from middle-late Ordovician to middle Silurian to cross the ancient equator (Figures 2B, C). The paleomagnetic poles of the middle-late Ordovician and Silurian further confirmed that a large southward apparent polar wander occurred in the Tarim block, which may be related to the significant northwestward movement and rotation of the Tarim block during the early Paleozoic (Sun and Huang, 2009).

By the end of the Silurian, the Tarim block had made a large drift to the northwest and completely broke away from the Gondwana supercontinent (Figure 2C, Huang et al., 2008, 2018; Zhao et al., 2018). This is consistent with the closure of the Kudi Ocean and the North Altyn Ocean on the southern margin of the Tarim block, in the late Ordovician-Silurian, and the collage events of the Central and South Kunlun terrane and the Altyn-Qilian terrane (Li et al., 2017). The late Ordovician to Silurian is the key period for the transition from N-S/T pattern to T-N/S pattern for the three blocks in China (Figure 2C, Zhao et al., 2018).

(2) The relationship between Tarim block and the surrounding block based on geological affinity

The South China block and Tarim block were at the same latitude in the early Paleozoic, and the changes of magnetic declination recorded by the two blocks were also similar, indicating that the two blocks were closely related in the early Paleozoic. In addition, the affinity between the two blocks and the Gondwana supercontinent, in the early Paleozoic, is supported by a large amount of geological and paleogeographic data (Huang et al., 2000; Sun and Huang, 2009).

The geological study shows that the South China block and the Tarim block are consistent in the spatial distribution of Sinian tillite, and there are strong similarities in Cambrian and Ordovician sediments, biota characteristics, and their temporal and spatial distribution, indicating that South China and Tarim blocks are closely related from Sinian to Ordovician (Zhu et al., 1998). Moreover, the age of basement formation and the early Paleozoic

metallogenic effects of the South China block and Tarim block show clear similarities to those of the Australia plate (Nie, 1991).

During the Ordovician period, the South China block, Tarim block, and Australia plate are very similar in the appearance of chitin and other paleontological groups, which are likely to belong to the “Pacific type” with high disparity (Duan and Ge, 1992; Chen and Wang, 1996; Duan and Ge, 2005; Sun and Huang, 2009). The paleogeographic study of trilobites shows that all of the North China block, South China block, and Australia plate belong to the Asian-Australian biological region, but there are significant differences between the North and South China blocks. In the comparison of the detrital zircon age spectrum, the South China and Tarim blocks have obvious differences with the North China block, which suggests that, even if the paleolatitude of these three blocks are very close (Huang et al., 2018), the North China block may be far away from other blocks in spatial location.

3 Database and methods

3.1 Database

The Tarim proto-type basin is an important research object. At present, the early Paleozoic maps of the Tarim Basin mainly include the tectonic-sedimentary environment maps compiled by Gao et al., 2016; Gao et al., 2017a; Gao et al., 2017b, the sedimentary model maps compiled by Chen et al., 2015, and the lithofacies paleogeographic maps provided by Tarim Oilfield Company.

The main data used include the residual thickness maps of Tarim Basin (Figure 3), the evolution maps of the equilibrium profile of Tarim Basin, the stratigraphic correlation maps of Tarim Basin, several seismic profiles (Figure 4 for example), and the peripheral margin shortening rate of Tarim Basin in Cenozoic (Jia et al., 2006; He et al., 2013; Chen et al., 2015; Tian et al., 2018; Laborde et al., 2019 and data from Tarim Oilfield Company).

3.2 Principles

The principles of proto-type basin recovery can be simply summarized as the following three aspects: the initial status, the practical process, and the real location (Lou et al., 2016; He et al., 2020; Liu et al., 2020), called P1, P2, and P3 hereafter.

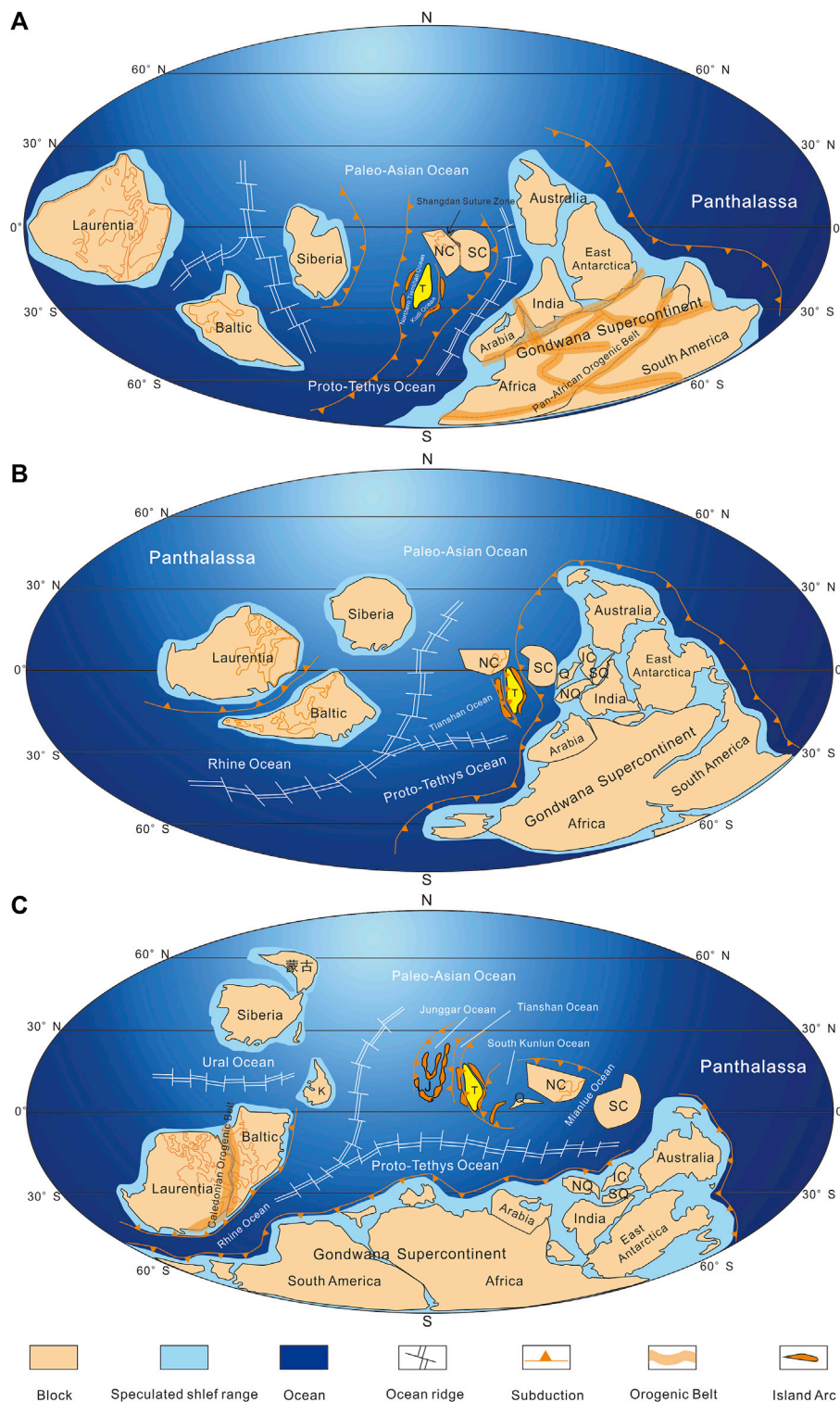


FIGURE 2 Reconstructing of global plates distribution in Cambrian Period (A), Ordovician Period (B), and Silurian Period (C). T-Tarim; NC-North China; SC-South China; Q-Qaidam; NQ-North Qiangtang; IC-Indochina; SQ-South Qiangtang; J-Junggar; K-Kazakhstan. (modified after Huang et al., 2018; Zhao et al., 2018).

P1 is to restore the scope and sedimentary facies distribution of the proto-type basin, and then analyze the type of the basin, including the uplift-depression pattern and sedimentary system of the proto-type basin, which needs to be restored on the basis of drilling, outcrop, seismic profile, and other basic data, especially the constraint

condition of the basin boundary and the recovery of denudation area (Tong and He, 2001; Zhang G. Y. et al., 2019; Zheng et al., 2021; Wang, p et al., 2021).

P2 is to restore the superposition transformation process of the proto-type basin, that is, the recovery of extension or shortening.

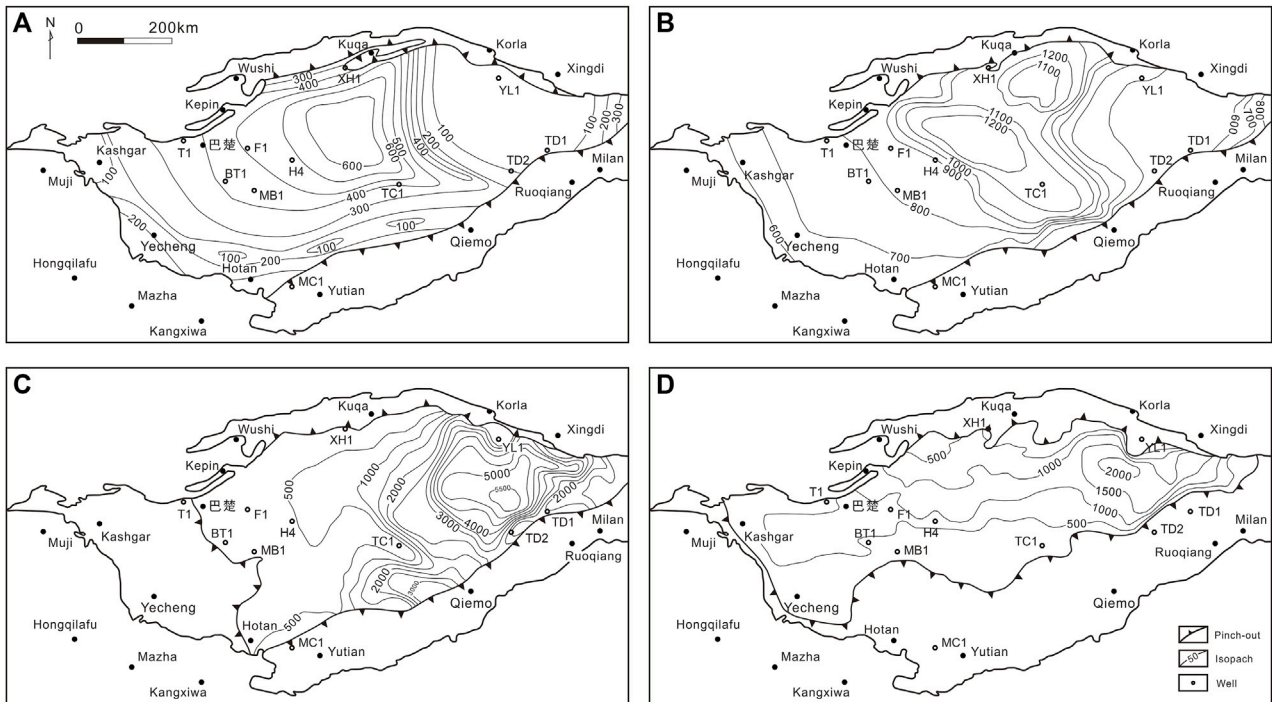


FIGURE 3 Residual thickness maps of Tarim in late middle-Cambrian (A), late Cambrian (B), late Ordovician (C), and late Silurian (D). (modified after [Chen et al., 2015](#) and data comes from Tarim Oilfield Company).

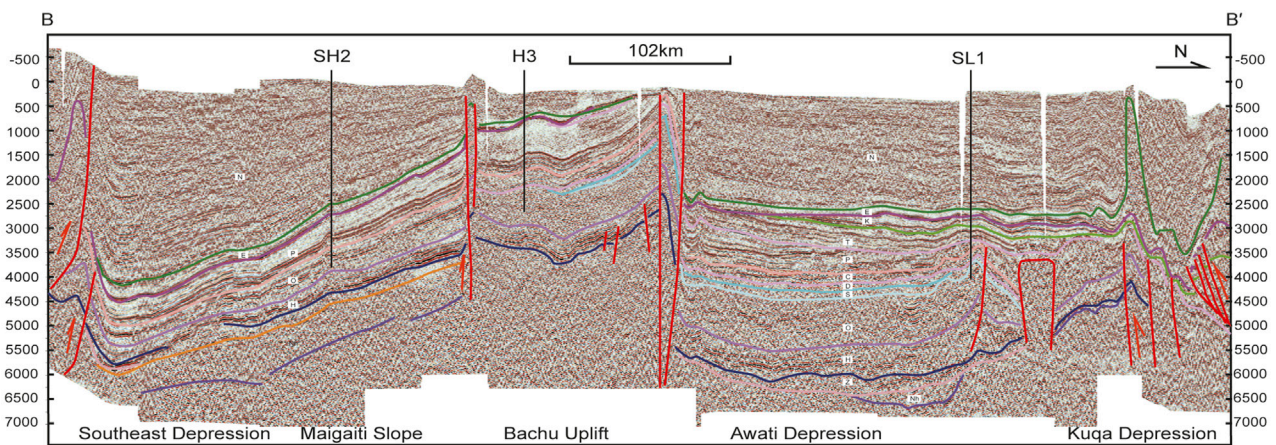


FIGURE 4 Geological interpretation of seismic section BB'. The location of this seismic section is shown in [Figure 1B](#).

Under the transformation of tectonics such as the Caledonian movement and Himalayan movement, there may be a great difference between the observed sedimentary range and the original sedimentary range, and the shortening can be calculated by the restoration of balanced cross sections ([Laborde et al., 2019](#)).

P3 is to restore the tectonic position during the development of the proto-type basin. On the one hand, to determine the paleo-position of the plate, that is, the paleolatitute, which can be measured and calculated by paleomagnetism ([Torsvik and Cocks, 2004](#); [Hou et al., 2020](#)) and analogy through the method of comparative tectonics; on the

other hand, the basin-mountain relationship is established by source-to-sink system analysis and clastic zircon analysis, which is useful for determining the relative position of the plate ([Hou et al., 2019](#); [Shao et al., 2019](#)).

3.3 Methods

The proto-type basin restoration methods for the Tarim Basin are mainly based on P1 and P2, and P3 is used to determine the location of

the Tarim block in the global plate tectonics. Detailed methods are described below.

- (1) The core point of the proto-type basin restoration lies in the scope of the proto-type basin. To determine the scope of the proto-type basin is to determine the boundary of the proto-type basin, which can be determined by the marginal facies method and the thickness trend method. The premise of using the marginal facies method is to clarify the type of the proto-type basin, different basins have different marginal facies, such as the marginal facies of lake basins are fan delta facies (Jiang, 2010; Ji et al., 2020; Wang and Lin, 2021). The thickness trend method can find the boundary of the proto-type basin with the help of the trend of the isopach in the isopach map, and it can also be analyzed by the trend surface of a certain thickness layer in the seismic profile (Zhang C, L et al., 2007; Yu et al., 2016). The residual thickness map is limited to the interior of the present Tarim Basin, so it is necessary to make up the isopach so as to restore the denudation area. The precondition of completing the isopach is to clarify the type of the proto-type basin, which can judge the opening and closing of the isopach. For example, the isopach of a rift basin is generally symmetric, while that of a foreland basin is asymmetric.
- (2) Restoring the original scope of the proto-type basin is indispensable, which means restoration to the state prior to shortening or expansion. The balanced cross-section method is to expand the scope of the proto-type basin after calculating the shortening by the balanced cross-section technique (Lou et al., 2016; Laborde et al., 2019).
- (3) According to the tectonic background analysis of the Tarim Basin, the island arc, terrane and ocean are placed on the peripheral margin of the Tarim Basin to show the oceanic-continental pattern. This step also needs to clarify the type of the peripheral basin of the Tarim block. If the basin is a passive continental margin basin, then the scope of the corresponding basin is relatively wide, and the terrane can be far away from the Tarim block; if the peripheral basin is an active continental margin, then the range of the basin is relatively narrower, and the terrane can be close to the Tarim block.

4 Result

4.1 Shortening amount of Tarim Basin

Laborde et al. (2019) made a detailed analysis of the shortening amount of Tarim Basin caused by various factors in the Cenozoic era (Table 2). Based on the statistical analysis of 81 profiles, in which 10 profiles (BB' for example, Figure 4) are recovered (Figure 5) by this study and 71 profiles provided by Tarim Oilfield Company, the shortening amount (Table 2) of 4 representative lateral lines (AA', BB', CC', DD', which are shown in Figure 1B), from early Paleozoic to pre-Cenozoic, are obtained.

Due to the influence of the Pamir Salient on the west side of the Tarim Basin, the shortening of the Tarim Basin gradually decreases from west to east, and the Cenozoic shortening rate accounts for the largest proportion of the total shortening rate in the western margin of the Tarim Basin, especially in the southwestern margin, up to 70% (southern margin of BB', Table 2). According to the calculated shortening rate of each side, the scope of the proto-type basin can be extended. It should be noted that the shortening amount of the Tarim Basin is mainly reflected in the margin of the Tarim Basin, which is shown visually on the outside of these two red dotted lines in Figure 5, and the impact on the interior of the Tarim Basin can be ignored.

4.2 Reconstruction of early Paleozoic proto-type Tarim Basin

Due to the long-term and complexity of geological evolution, the original proto-type basin will experience many tectonic actions of different properties. During these tectonic processes, the uplifting pattern, basin properties, and distribution of sedimentary facies in the Tarim Basin have undergone great change, which play important roles in hydrocarbon accumulation, migration, and trap (Lin et al., 2008). Through the analysis of residual basin fillings and tectonic background, restoring the proto-type of the basin and analyzing the later transformation is of great significance to understand the distribution of petroleum reservoirs in the superimposed basin (Wang et al., 2010; Chen et al., 2017).

TABLE 2 Shortening amount of Tarim Basin from Cenozoic, Silurian, Ordovician, Cambrian to the present (km).

Distribution of the shortening amount	Cenozoic (Laborde et al., 2019)	Silurian (this study)	Ordovician (this study)	Cambrian (this study)
Northern margin of AA'	36.0	54.0	65.0	64.0
Southern margin of AA'	32.0	46.0	50.0	50.0
Northern margin of BB'	21.0	43.0	50.0	47.0
Southern margin of BB'	35.0	50.0	54.0	50.0
Northern margin of CC'	22.0	39.0	45.0	42.0
Southern margin of CC'	0.9	15.0	20.0	16.0
Northern margin of DD'	0.0	15.0	23.0	23.0
Southern margin of DD'	0.3	24.0	36.0	33.0

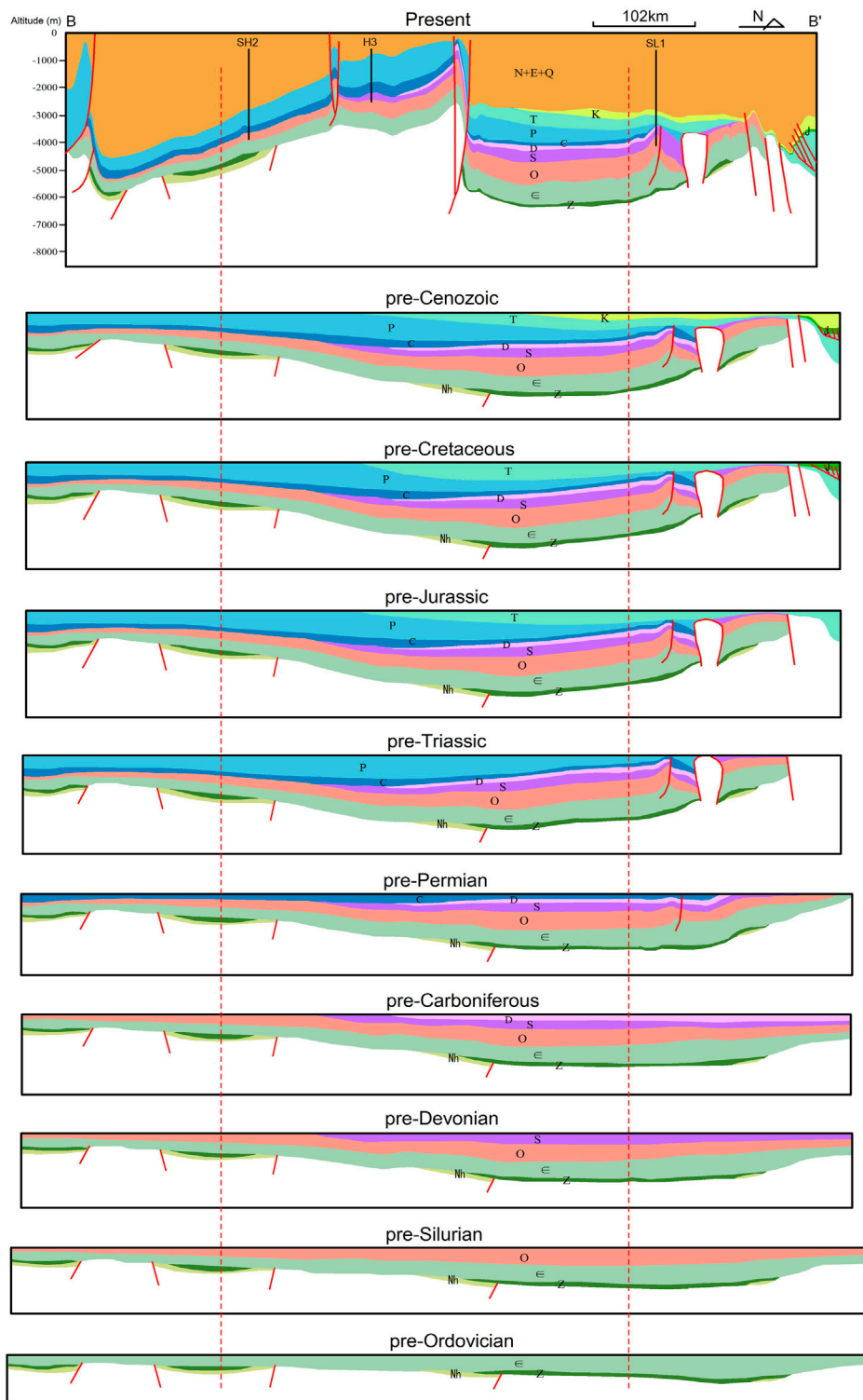
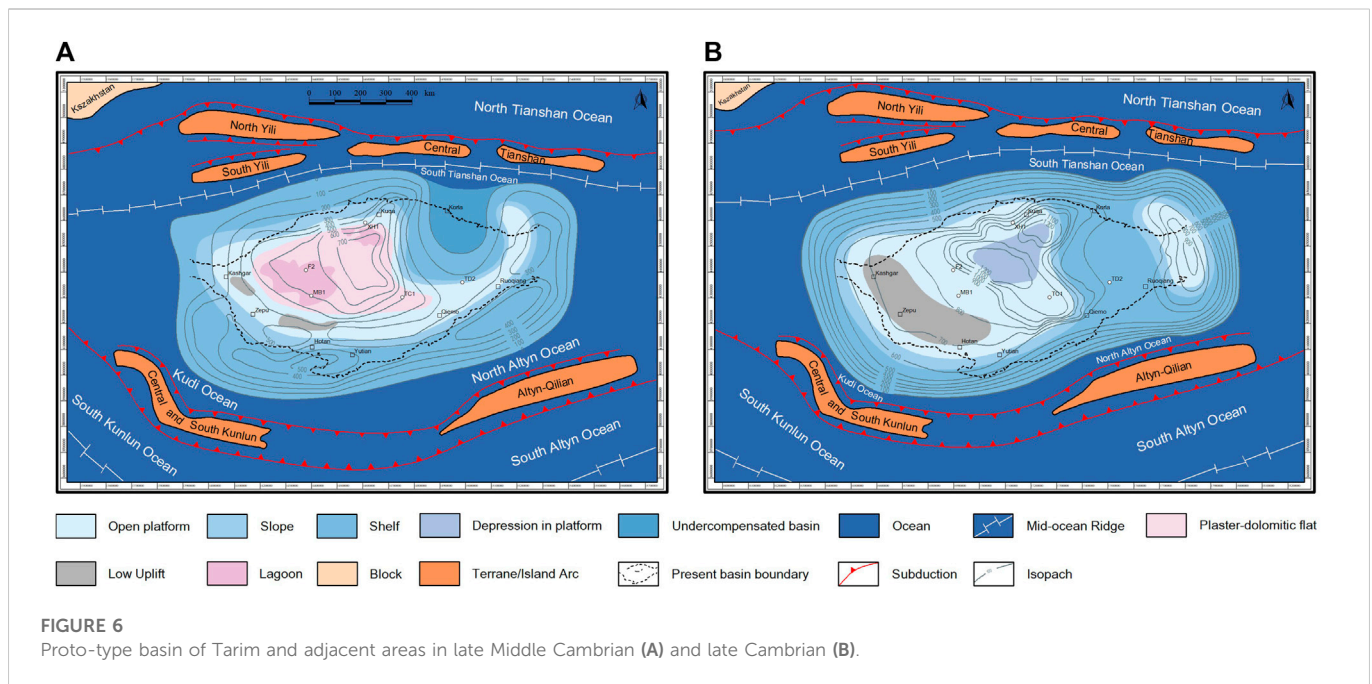


FIGURE 5 Recovered balanced cross-section of BB'. The location of this seismic section is shown in Figure 1B. The red dotted lines visually represent the boundary between the margin and the interior of the Tarim Basin.

(1) Proto-type Tarim Basin in late Middle Cambrian

In the Middle Cambrian, the Tarim Basin was mainly controlled by the extensional tectonic environment (Lin et al., 2008; Yun et al., 2014). The South Tianshan Ocean is in a stage of

continuous expansion, with the South Tianshan intercontinental rift developed in the northern margin of the Tarim Basin. Meanwhile, the Kudi Ocean and the North Altyn Ocean, located in the southern margin of the Tarim Basin, reached the maximum range (Figure 6A).



Under the extensional background, the internal uplift-depression pattern of the Tarim Basin changes from north-south differentiation to east-west differentiation, with the embryonic form of “carbonate platform in the west, deep-water basin in the east” appearing (Chen et al., 2015; Li et al., 2015; Gao et al., 2017a). In the western part of the Tarim Basin, the intracratonic basin, characterized by restricted platform sedimentation, widely developed plaster-salt rock facies (Figure 6A), which are good reservoir strata, while the cratonic marginal basin in the eastern part of the Tarim Basin, featured on deep-water deposits, developed siliceous-bearing mudstone (Gao, 2015; Zhang et al., 2015; Wu et al., 2016; Gao et al., 2017a) and has not yet achieved north-south penetration in space (Figure 6A). On the whole, the ramp - evaporate platform - platform margin - slope - deep-water facies model (Chen et al., 2015; Tian et al., 2018) was developed in the Tarim Basin during the middle Cambrian. Passive continental margin basin is developed in both the southern and northern margin of the Tarim Basin, especially the passive continental margin basin in the southwest of the Tarim Basin, where the shelf facies have a wide distribution range, which is beneficial to hydrocarbon generation.

(2) Proto-type Tarim Basin in late Cambrian

In the late Cambrian, as a whole, it inherited the basin pattern of the middle Cambrian (Figure 6B), which was still controlled by the extensional tectonic environment (Lin et al., 2008; Yun et al., 2014). The South Tianshan Ocean, in the northern margin of the Tarim Basin, continued to expand, while the Kudi Ocean and Albyn Ocean in the southern margin of the Tarim Basin were getting narrow (Figure 6B).

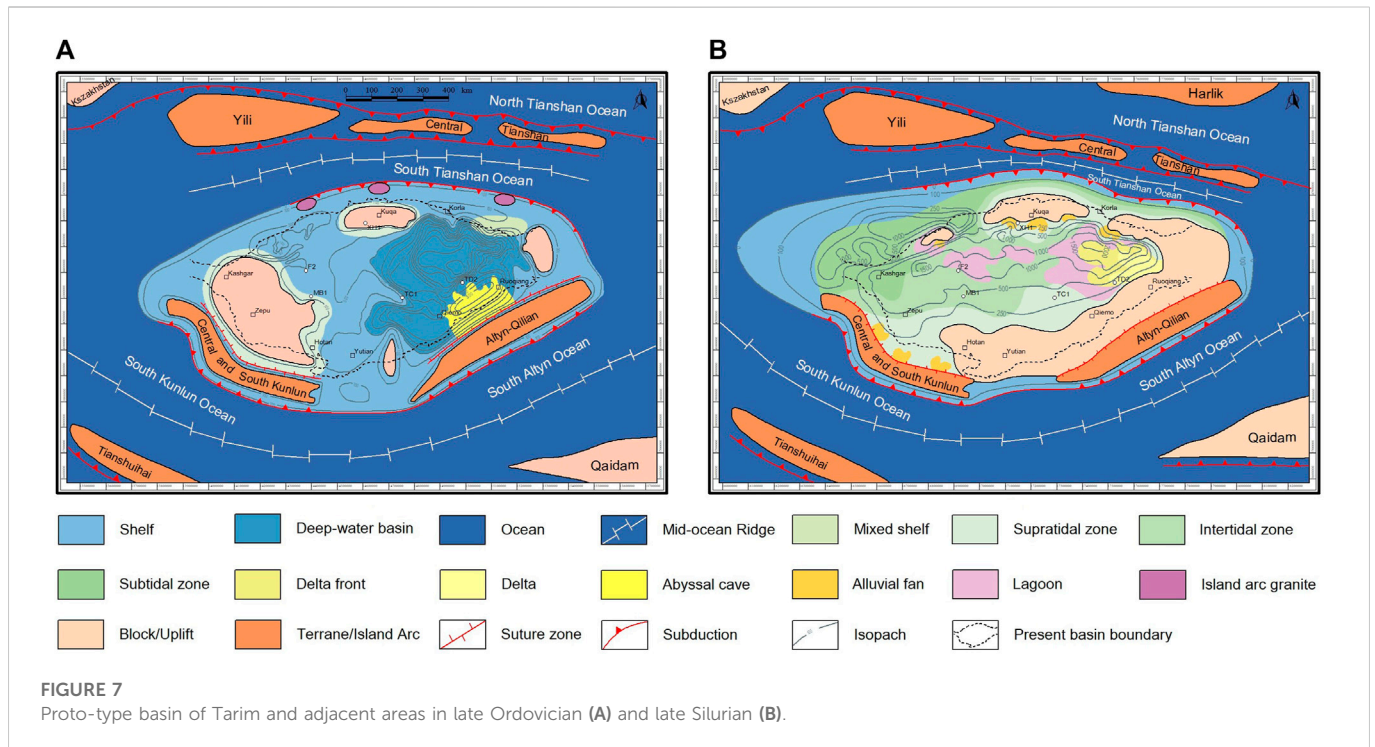
At the end of the late Cambrian, the cratonic marginal basin in the eastern part of the Tarim Basin achieved north-south penetration in space, and the paleogeographic pattern “east-west differentiation” was completely formed (Gao et al., 2012; Gao et al., 2017a). The platform formation developed in the west, dominated by open-platform

deposition, while in the east it was dominated by deep-water basin facies deposition (Figure 6B, Zhang et al., 2015; Wu et al., 2016; Gao et al., 2017a). As a whole, the restricted platform—semi-restricted platform—open platform—platform margin—slope—deep-water facies model (Chen et al., 2015) was developed in the Tarim Basin during the late Cambrian. Compared with the early Middle Cambrian (Figure 6A), the main change in the late Cambrian is the disappearance of evaporate platform facies, transforming to semi-restricted and restricted platform, which indicates that the relative sea level of the late Cambrian gradually rose and the water body deepened slowly, with the plaster-salt rock facies vanishing (Figure 6B). Passive continental margin basins still developed in the southern and northern margin of the Tarim Basin, the former becoming wider and the latter narrowing due to the subduction of the Kudi Ocean and the North Albyn Ocean.

(3) Proto-type Tarim Basin in late Ordovician

In the middle-late Ordovician, the subduction of the Kudi Ocean and the North Albyn Ocean led to the transformation of the tectonic environment from extension to compression in the southern margin of the Tarim Basin (Lin et al., 2008; Yun et al., 2014; Li et al., 2015; Zhang L. N. et al., 2019; Wu et al., 2021). At the end of the Ordovician, the South Tianshan Ocean reached the maximum, then subducted northward to the Central Tianshan and Yili terranes and southward to the Tarim block (Figure 7A, Lin et al., 2012; Jiang et al., 2014).

In the Ordovician, under the influence of the subduction of the Kudi Ocean and the North Albyn Ocean, the uplift-depression pattern of the Tarim Basin changed from east-west differentiation to north-south differentiation (Figure 7A, Lin et al., 2012; Yun et al., 2014; Gao et al., 2016; Gao et al., 2017b), and the peripheral uplift of the Tarim Basin was obvious, especially in the southwest of the Tarim Basin, with the depocenter of the basin migrating to the Manjiaer Depression and the Tabei Uplift surfaced for the first time (Figure 7A). The



intracratonic basin developed in the middle of the Tarim Basin, and the back-arc foreland basin (Figure 7A) developed in the southeast and southwest margin of the Tarim Basin, which gradually disappeared under the injection of abundant provenances at the end of Ordovician (Gao et al., 2017b).

(4) Proto-type Tarim Basin in late Silurian

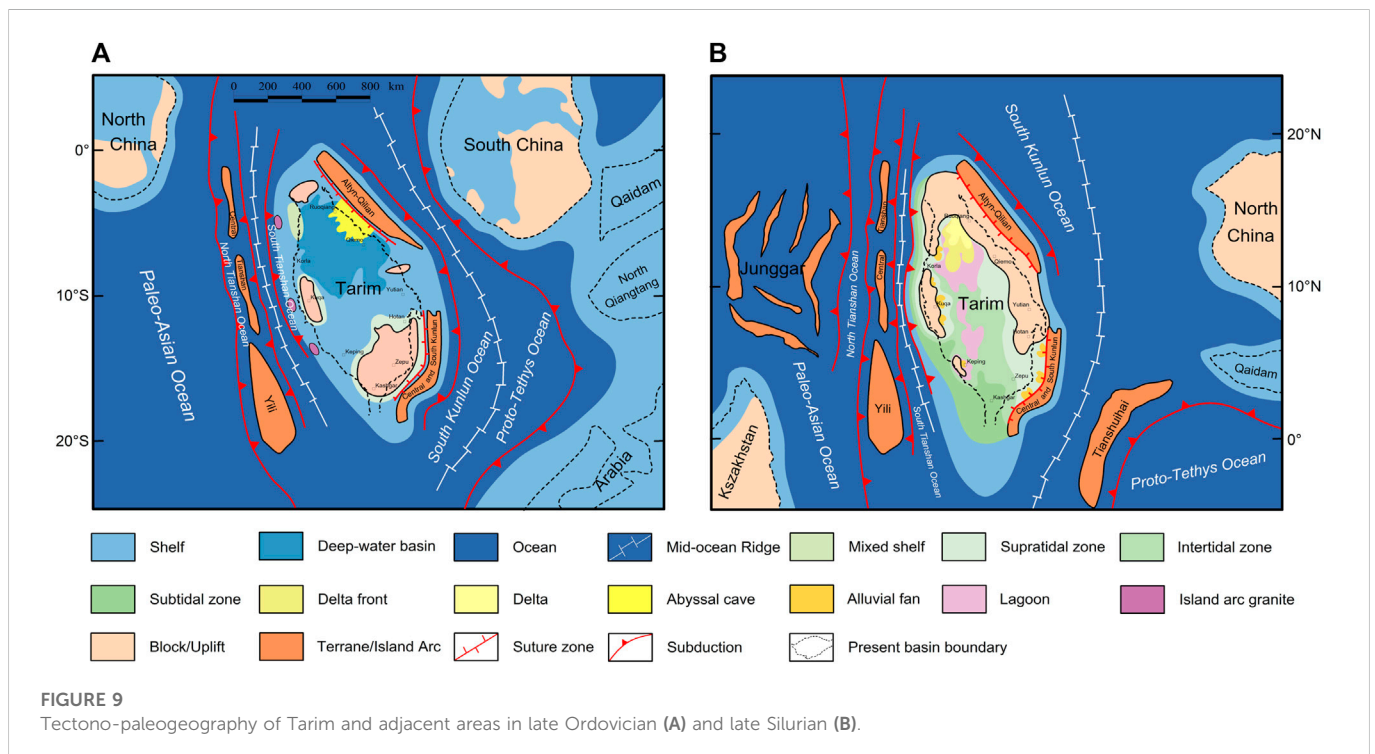
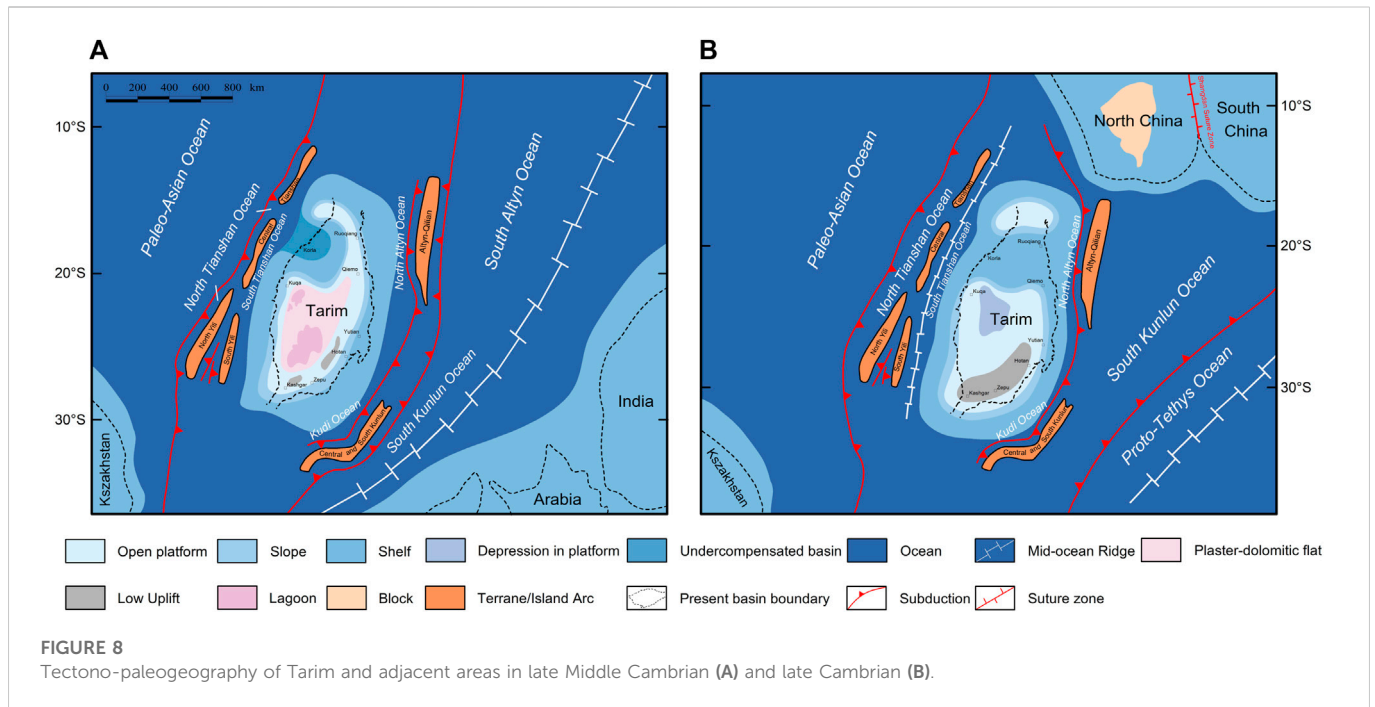
The continuous collision of the Central and South Kunlun and Alтын-Qilian terraces with the Tarim block during the Silurian period resulted in a strong compression of the Tarim Basin, with the South Kunlun Ocean, the South Alтын Ocean, and the South Tianshan Ocean continuing to subduct (Figure 7B, Xu et al., 2011; Li et al., 2015; Wu et al., 2021).

During the Silurian, uplifts developed in the south, north, and east of the Tarim Basin, with depression in the middle (Figure 7B, Lin et al., 2011; Lin et al., 2012; He et al., 2013; Zheng et al., 2014). Topographically, the Tarim Basin is high in the south and low in the north, developing intracratonic depression in the central basin, which provenances are mainly from the eastern and southeastern margins of the Tarim Basin (Figure 7B, Jia et al., 2006; Lin et al., 2011). The shallow sea in the west of the Tarim Basin is open, and the east is blocked with the transgression mainly coming from the north and northwest (Jia et al., 2006; Lin et al., 2011; Li et al., 2015), and the lithofacies paleogeographic pattern of shelf - subtidal - intertidal - supratidal facies is developed from northwest to southeast (Figure 7B, Wu et al., 2020). The back-arc foreland basins in the southeastern and southwestern margin of the Tarim Basin have been extinct, and the Tanan Uplift developed under the background of extrusion.

4.3 Reconstruction of early Paleozoic tectono-paleogeography around the Tarim basin

In the middle Cambrian, the North Alтын Ocean, in the southeast margin of the Tarim block, and the Kudi Ocean, in the southwest margin, began to subduct southward, and the Central and South Kunlun and Alтын-Qilian terrane began to approach the Tarim block (Figure 8A, Gao et al., 2017a; Mou et al., 2018). The South Tianshan Ocean on the northern margin of the Tarim Basin continued to expand, the Yili and Central Tianshan terranes were far away from the Tarim Basin, while the North Tianshan Ocean continued to subduct southward beneath the Yili and Central Tianshan terranes (Figure 8A). It should be noted that the Yili terrane was an arc-basin system, which was divided into North and South Yili, until the end of the Ordovician (Figure 8A, B, Figure 9A, Wang et al., 2012; Wang et al., 2014a; Wang et al., 2014b; Huang et al., 2021). At the end of the middle Cambrian, the Arabian and Indian blocks had not yet been separated from the Gondwana supercontinent, all in a shallow sea environment, dominated by carbonate deposits (Li et al., 2013; Rao et al., 2016), while the Kazakhstan block was free outside the Gondwana, but also developed shallow marine deposits (Shen et al., 2016; Zhang G. Y. et al., 2019).

During the Cambrian period, the Tarim block and surrounding blocks were still controlled by the extensional tectonic environment (Lin et al., 2008; Yun et al., 2014). The North Alтын Ocean and the Kudi Ocean continued to subduct southward, thus the North Alтын Ocean and the Kudi Ocean further narrowed, with the Central and South Kunlun and Alтын-Qilian terrane closer to the Tarim block (Figure 8B). From a more macro perspective, the Paleo-Asian Ocean and the Proto-Tethys Ocean were also subducting towards the Tarim block (Figure 8B, Zhao et al., 2018). At the end of the Cambrian, driven



by the subduction of the Shangdan Ocean, the North China block collided with the South China block, which formed the Shangdan suture zone and developed uplifts in the interior of the North and South China blocks (Chen and Liu, 2011; Li and Jiang, 2013, Lin et al., 2016), with shallow marine deposits in the periphery (Hu et al., 2022; Zhang G. Y. et al., 2019; Zhang et al., 2019).

In the Ordovician, except for the Gondwana Supercontinent, all the other landmasses drifted northward, and the Tarim, South China,

and North China blocks also drifted to low latitudes (Figure 9A, Huang et al., 2018; Zhao et al., 2018). The South China and North China blocks separated again, and the latter drifted westward relative to the Tarim block, accompanied by clockwise rotation (Figure 9A, Huang et al., 2018; Zhao et al., 2018). The Tarim block and its surrounding areas are under compression environment, and part of the South and North China blocks have developed large-scale uplifts, other areas developing shallow marine deposits with the Qaidam

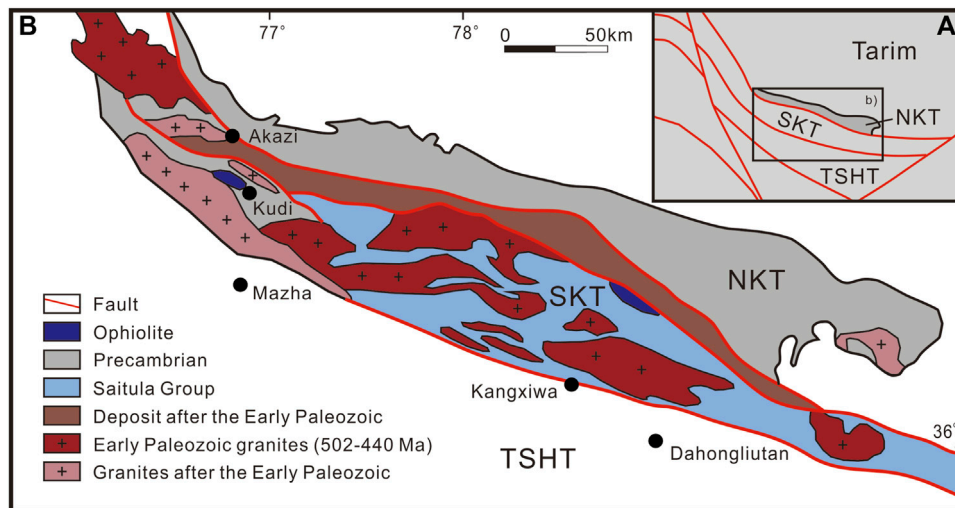


FIGURE 10
Location (A) and tectonic framework (B) of the West Kunlun orogenic belt and its adjacent areas (NKT: The North Kunlun terrane, which is a part of the Tarim block; SKT: The South Kunlun terrane, which can correspond to the Central and South Kunlun terrane in early Paleozoic; TSHT: The Tianshuihai terrane) (modified after Zhang L. N. et al., 2019).

terrane, North Qiangtang terrane, and the northwestern margin of the Arabian Plate, located on the margin of the Gondwana (Figure 9A, Feng et al., 2004; Li et al., 2013; Chen et al., 2015; Zhou et al., 2017; Zhang G. Y. et al., 2019). Until the end of the Ordovician, the middle Caledonian movement led to the closure of the Kudi Ocean and the North Altyn Ocean (Figure 9A, Lin et al., 2008; Yun et al., 2014; Li et al., 2015; Zhang L. N. et al., 2019; Wu et al., 2021). The Central and South Kunlun and Altyn-Qilian terranes collided with the Tarim block, while the Tianshuihai-Bayanhar terrane and Qaidam block approached the Tarim block (Mou et al., 2018; Zhang L. N. et al., 2019). At the same time, the South Tianshan Ocean began to subduct southward beneath the Tarim block and northward beneath the Yili and Central Tianshan terranes (Figure 9A, Zhou et al., 2004; Wang et al., 2009; Ge et al., 2012; Lin et al., 2012; Jiang et al., 2014).

During the Silurian period, the position of the three blocks in China was relatively discrete, and the North China block was uplifted into a denudation area (Figure 9B), which was the same as the Kazakhstan, Arabian and Indian plates, while the South China block developed shallow marine deposits as a whole, which was located on the eastern side of the North China block (Huang et al., 2018; Zhao et al., 2018; Zhang G. Y. et al., 2019). The Tarim block is relatively isolated, and the shallow marine deposits are mainly developed in the northwest of the Tarim block (present location, Figure 7B, Figure 9B, Lin et al., 2011; Lin et al., 2012; He et al., 2013; Zheng et al., 2014; Li et al., 2015). The Qaidam terrane between the Tarim and North China terranes also develops shallow marine deposits (Figure 9B, Zhang G. Y. et al., 2019). At the end of the Silurian, the Central and South Kunlun and Altyn-Qilian terranes completely merged with the Tarim block, forming a larger Tanan uplift, and the South Kunlun Ocean and the South Altyn Ocean continued to submerge northward, with the Tianshuihai-Bayanhar terrane and Qaidam block closer to the Tarim block (Figure 9B, Xu et al., 2011; Li et al., 2015; Wu et al., 2021). It should be noted that in the north of the Tarim block (present location) and the east of the

Kazakhstan plate, the Junggar arc group has not been collaged to form the Junggar terrane (Figure 9B, Xiao et al., 2010; Carmichael et al., 2019).

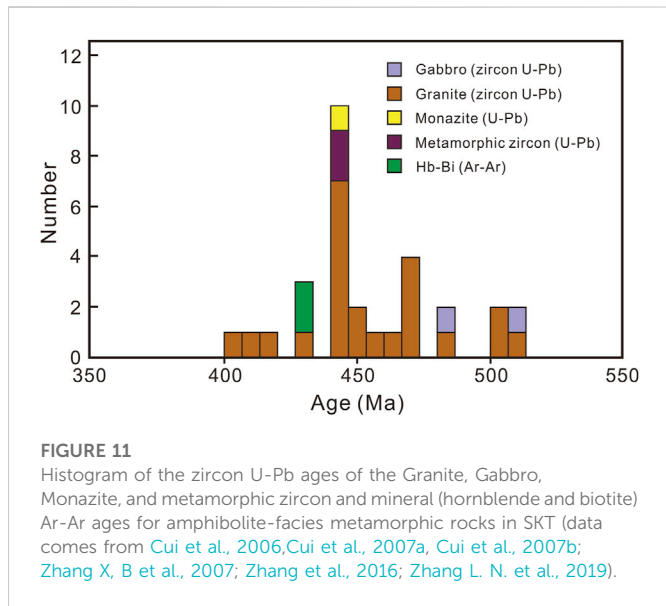
5 Discussion

In the early Paleozoic, the periphery of the Tarim Basin was greatly changed, especially the appearance, expansion, and closure of the Kudi Ocean and North Altyn Ocean on the southern margin, transforming the tectonic environment of the Tarim Basin from extension to extrusion, which changed the scope and nature of the proto-type basin. To determine the peripheral background of the Tarim Basin in the early Paleozoic, the focus is on when the peripheral oceans of the Tarim Basin were opened and closed, and when the surrounding terranes collided.

5.1 The expansion and closure of the Kudi Ocean

The Kudi ophiolite exposed in the West Kunlun orogenic belt is evidence of the existence of the early Paleozoic Kudi Ocean between the Tarim Basin and the Central and South Kunlun terrane in the southwest margin of the Tarim Basin (Zhang L. N. et al., 2019).

Through the spatial relationship between ophiolite and granite in the same period, the subduction direction of the Kudi Ocean can be judged, and then the nature of the southwest peripheral basin of the Tarim Basin can be determined (Zhang L. N. et al., 2019). The residual ophiolite in the northern margin of the Saitula Group and the granite developed on SKT in the early Paleozoic (Figure 10) indicate that the Kudi Ocean subducted southward to the Central and South Kunlun terrane (Figures 8, 10), thus the passive continental margin basin develops at the southwest margin of



the Tarim Basin, which is a good place for the development of hydrocarbon resources.

The age of the gabbro in the Kudi ophiolite is concentrated between 510 and 525 Ma (Xiao et al., 2003; Zhang et al., 2004; Fang et al., 2010), indicating that the Kudi Ocean was in the stage of oceanic expansion in the early-middle Cambrian. The Tiekeli Formation of the NKT contains a mass of middle-late Ordovician granodiorite (Matte et al., 1996), showing that the NKT is the collisional orogenic belt in the middle-late Ordovician.

The zircon U-Pb ages of the granite, monazite, and metamorphic zircons, and the Ar-Ar ages for hornblende and biotite in the amphibolite-facies metamorphic rocks in SKT are concentrated in 450–440 Ma (Figure 11, Cui et al., 2006, Cui et al., 2007a, Cui et al., 2007b; Zhang X B et al., 2007; Zhang et al., 2016; Zhang et al., 2019b), which means that the collision period of the

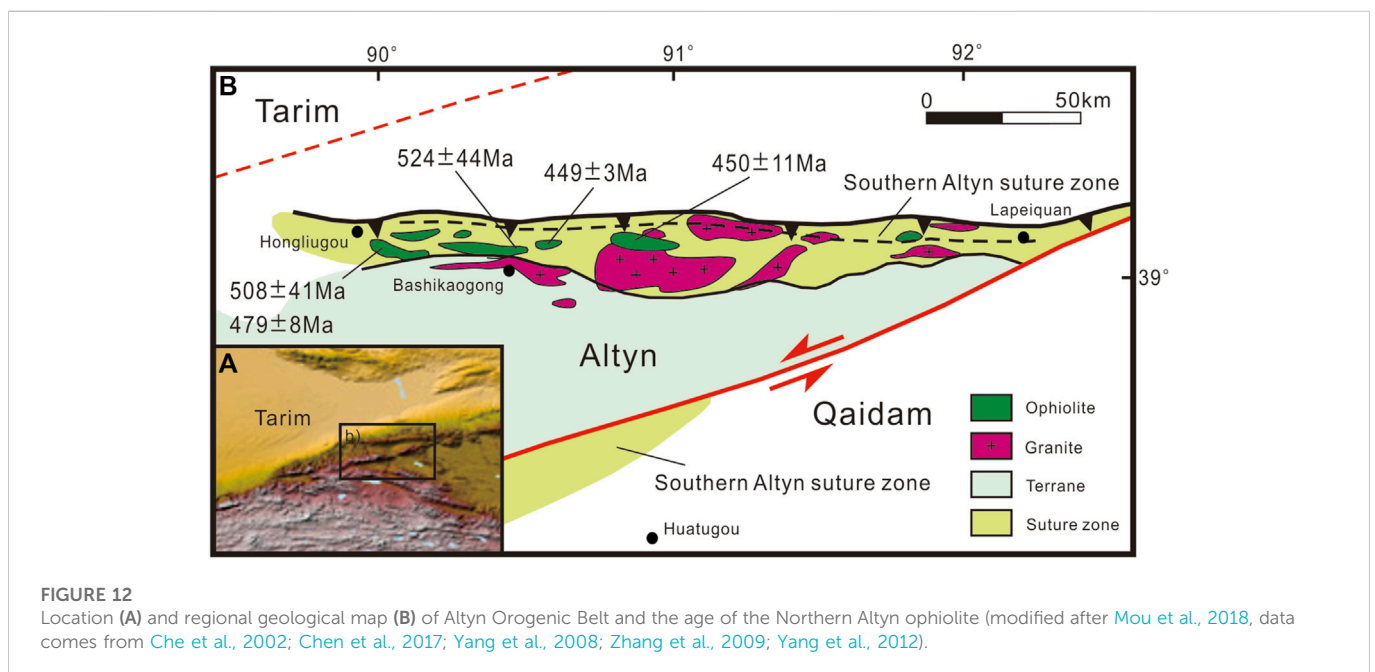
SKT is 450–440 Ma, that is, in the late Ordovician, the Central and South Kunlun terrane collage up and the Kudi Ocean closed (Figure 9A, Zhang L. N. et al., 2019).

5.2 The expansion and closure of the North Altyn Ocean

The Hongliugou-Lapaiquan ophiolite in the Northern Altyn suture zone is evidence of the existence of the North Altyn Ocean (Mou et al., 2018), which is located in the southeastern margin of the Tarim Basin and between the Tarim Basin and the Altyn-Qilian terrane in the early Paleozoic. There are two areas of concentrated ophiolites in the Altyn orogenic belt, called the Hongliugou-Lapaiquan ophiolite belt and the Apa-Mangya ophiolite belt, corresponding to the Northern Altyn suture zone and the Southern Altyn suture zone, respectively, and the Altyn-Qilian terrane is sandwiched between two suture zones (Figure 12, Sobel and Araud, 1999; Xu et al., 1999; Meng et al., 2010).

The formation age of the Northern Altyn metamorphic rocks in Hongliugou is concentrated in the Middle-late Cambrian (Mou et al., 2018), indicating that the North Altyn Ocean began to subduct in the Middle-late Cambrian, and the age of the Northern Altyn ophiolite is concentrated in 524–449 Ma (Figure 12, Che et al., 2002; Chen et al., 2015; Yang et al., 2008; Zhang et al., 2009; Yang et al., 2012), indicating that the closure of the North Altyn Ocean should not be earlier than 449 Ma. In addition, in Hongliugou and other places, there are granites formed in the subduction environment in the late Cambrian-late Ordovician (500–443 Ma) (Chen et al., 2003; Kang et al., 2011) and granites representing syn-collision and post-collision setting in the Ordovician-late Silurian (474–419 Ma) (Wu et al., 2005, 2007; Yang et al., 2012).

Based on the geochemical study of the intermediate-acid volcanic rocks in the Altyn orogenic belt, it is found that the granites, from south to north, have the characteristic of the transition from I-type granite to S-type granite, indicating that the North Altyn Ocean



subducted to the Altyn-Qilian terrane in the early Paleozoic (Figure 8, Li et al., 2013).

5.3 Two-direction subduction of the South Tianshan Ocean

At the beginning of the early Paleozoic, the Tarim block was separated from the Rodinia supercontinent. The continental rift basalts were developed in the Lower Cambrian of the Kuruketage, Keping, and South Tianshan areas (Jia, 1997; Li et al., 2006), representing the extensional movement on the northern margin of the Tarim block in the Cambrian and the emergence of the South Tianshan Ocean between the Central Tianshan terranes and the Tarim block. Until the early Carboniferous period, there were still new oceanic crusts formed in the South Tianshan Ocean (Jiang et al., 2014).

According to the traditional view, the northward subduction of the South Tianshan Ocean lasted from the late Ordovician to the late Carboniferous, while the northern margin of the Tarim Basin was always a passive continental margin environment, thus continuously developing thick layers of Paleozoic sediments (Zhou et al., 2004; He et al., 2007; Li et al., 2010; Wang et al., 2011). However, in recent years, several medium-acidic intrusive rocks have been discovered near the northern margin of the Tarim Basin, and the U-Pb zircon ages of these medium-acidic intrusive rocks are concentrated in the late Ordovician-early Silurian, indicating the southward subduction of the South Tianshan Ocean at the same time (Figure 9A, Wang et al., 2009; Ge et al., 2012; Lin et al., 2012; Jiang et al., 2014). In other words, the northern margin of the Tarim Basin has changed from passive continental margin to active continental margin at the end of the Ordovician period (Figure 9A).

6 Conclusion

- (1) Due to the influence of the Pamir Salient, the shortening of the Tarim Basin gradually decreases from west to east, and the Cenozoic shortening rate accounts for the largest proportion of the total shortening rate in the western margin of the Tarim Basin. The shortening amount of the Tarim Basin is mainly reflected in the margin of the Tarim Basin, and the impact on the interior of the Tarim Basin can be ignored.
- (2) In the Cambrian, the Tarim Basin was mainly controlled by the extensional tectonic environment, with the sedimentary framework of “carbonate platform in the west, deep-water basin in the east”. During the middle-late Ordovician, the subduction of the Kudi Ocean and the North Altyn Ocean led

to the transformation of the tectonic environment from extension to compression in the southern margin of the Tarim Basin, thus the uplift-depression pattern of the Tarim Basin changed from east-west differentiation to north-south differentiation.

- (3) The North Altyn Ocean and the Kudi Ocean began to subduct southward beneath the Central and South Kunlun and Altyn-Qilian terranes in the middle Cambrian. Until the end of the Ordovician, under the influence of the middle Caledonian movement, the two oceans closed, and the Central and South Kunlun and Altyn-Qilian terranes collided with the Tarim block, which greatly changed the uplift-depression pattern, basin properties, and sedimentary facies distribution of the Tarim Basin.

Data availability statement

The original contributions presented in the study are included in the article/Supplementary Material, further inquiries can be directed to the corresponding author.

Author contributions

ZZ did most of the job in this article, including literature review, balanced cross-section recovery, manuscript writing, drawing of maps and so on; SH and CL generously offered the main data used in this article, HC, JX, XL, and LW contributed to the reconstruction of early Paleozoic proto-type Tarim Basin; HZ helped a lot in reconstructing global plates distribution.

Conflict of interest

SH and CL were employed by Tarim Oilfield Company.

The remaining authors declare that the research was conducted in the absence of any commercial or financial relationships that could be construed as a potential conflict of interest.

Publisher's note

All claims expressed in this article are solely those of the authors and do not necessarily represent those of their affiliated organizations, or those of the publisher, the editors and the reviewers. Any product that may be evaluated in this article, or claim that may be made by its manufacturer, is not guaranteed or endorsed by the publisher.

References

- Cao, W. C., Zahirovic, S., Flament, N., Williams, S., Golonka, J., and Müller, R. D. (2017). Improving global paleogeography since the late Paleozoic using paleobiology. *Biogeosciences* 14, 5425–5439. doi:10.5194/bg-14-5425-2017
- Carmichael, S. K., Waters, J. A., Königshof, P., Suttner, T. J., and Kido, E. (2019). Paleogeography and paleoenvironments of the late devonian kellerwasser event: A review of its sedimentological and geochemical expression. *Glob. Planet. Change* 183, 102984. doi:10.1016/j.gloplacha.2019.102984
- Che, Z. C., Liu, L., and Luo, J. H. (2002). *Regional tectonics of China and its adjacent regions*. Beijing: Science Press, 07–369. (in Chinese).
- Chen, D. L., and Liu, L. (2011). New data on the chronology of eclogite and associated rock from Guanpo Area, North Qinling orogeny and its constraint on nature of North Qinling HP-UHP eclogite terrane. *Earth Sci. Front.* 18, 158–169. (in Chinese with English abstract).
- Chen, H. D., Hou, M. C., Chen, A. Q., Shi, Z. Q., Xing, F. C., Huang, K. K., et al. (2017). Research progress and key scientific problems of palaeogeography in China. *Acta Sedimentol. Sin.* (05), 888–901. (in Chinese). doi:10.14027/j.cnki.cjxb.2017.05.003
- Chen, X. H., Gehrels, G., Wang, X. F., Yang, X. F., Yang, F., and Chen, Z. L. (2003). Discussion on the formation age and tectonic environment of granite in the northern

- margin of Altyn Mountain. *Bull. Mineralogy, Petrology Geochem.* 22 (4), 294–298. (in Chinese). doi:10.3969/j.issn.1007-2802.2003.04.002
- Chen, X. H., Wang, X. F., and Li, Z. H. (1996). Arenigian chitinozoan biostratigraphy and paleobiogeography in South China. *Geol. Rev.* 42 (3), 200–208. (in Chinese). doi:10.3321/j.issn:0371-5736.1996.03.002
- Chen, X. W., Mou, C. L., Zhou, K. K., Kang, J. W., Wang, Q. Y., Ge, X. Y., et al. (2015). Lithofacies and palaeogeography of ordovician in north China. *Sediment. Geol. Tethyan Geol.* 35 (04), 1–11. (in Chinese).
- Chen, Y. Q., Yan, W., Han, C. W., Yang, P. F., and Li, Z. (2015). Redefinition on structural paleogeography and lithofacies paleogeography framework from cambrian to early ordovician in the Tarim Basin: A new approach based on seismic stratigraphy evidence. *Nat. Gas. Geosci.* 26 (10), 1831–1843. (in Chinese). doi:10.11764/j.issn.1672-1926.2015.10.1831
- Cocks, L. R. M., and Torsvik, T. H. (2002). Earth geography from 500 to 400 million years ago: A faunal and palaeomagnetic review. *J. Geol. Soc.* 159, 631–644. doi:10.1144/0016-764901-118
- Cui, J. T., Bian, X. W., and Wang, G. B. (2006). Geological composition and evolution of the West Kunlun. *Geol. Shaanxi* 24, 1–11. doi:10.1016/j.gsf.2018.05.006
- Cui, J. T., Wang, J. C., Bian, X. W., Luo, Q. Z., Zhu, H. P., Wang, M. C., et al. (2007a). Zircon SHRIMP U-Pb dating of the dongbake gneissic tonalite in the northern kangxiwa, West Kunlun. *Geol. Bull. China* 26, 726–729. (in Chinese with English abstract). doi:10.3969/j.issn.1671-2552.2007.06.014
- Cui, J. T., Wang, J. C., Bian, X. W., Zhu, H. P., Luo, Q. Z., Yang, K. J., et al. (2007b). Zircon SHRIMP U-Pb dating of early Paleozoic granite in the Mengguobao-Pushou area on the northern side of the Kangxiwa, West Kunlun. *Geol. Bull. China* 26, 710–719. (in Chinese with English abstract). doi:10.3969/j.issn.1671-2552.2007.06.012
- Dong, Y. P., He, D. F., Sun, S. S., Liu, X. M., Zhou, X. H., Zhang, F. F., et al. (2018). Subduction and accretionary tectonics of the East Kunlun Orogen, Western segment of the central China orogenic system. *Earth-Science Rev.* 186, 231–261. doi:10.1016/j.earscirev.2017.12.006
- Duan, J. Y., and Ge, X. H. (2005). Stratigraphic and paleobiogeographic affinities between different tectonic units in northwestern China-With a discussion of the tectonic framework of northwestern China. *Geol. Bull. China* 24 (6), 558–563. (in Chinese with English abstract). doi:10.3969/j.issn.1671-2552.2005.06.013
- Duan, J. Y., and Ge, X. H. (1992). Tarim-Yangzi and its paleogeographic pattern. *J. Changchun Univ. Earth Sci.* 22 (3), 260–268. (in Chinese).
- Fang, A. M., Li, J. L., and Chu, Z. Y. (2010). Sm-Nd isochron age of basic volcanic rocks in Kudi ophiolite, West Kunlun. *Chin. J. Geol.* 45 (01), 113–121. (in Chinese). doi:10.3969/j.issn.0563-5020.2010.01.011
- Fang, D. J., Jin, G. H., Jiang, L. P., Wang, P. Y., and Wang, Z. L. (1996). Paleozoic paleomagnetic results and the tectonic significance of Tarim Plate. *Chin. J. Geophys.* 39 (4), 522–532. (in Chinese with English abstract). doi:10.3321/j.issn:0001-5733.1996.04.010
- Feng, Z. Z., Peng, Y. M., Jin, Z. K., and Bao, Z. D. (2004). Lithofacies palaeogeography of the late ordovician in China. *J. Palaeogeogr.* 02, 127–139. (in Chinese with English abstract). doi:10.3969/j.issn.1671-1505.2004.02.001
- Gao, H. H., He, D. F., Tong, X. G., Wen, Z. X., Wang, Z. M., and He, J. Y. (2016). Tectonic-depositional environment and proto-type basins during the depositional period of middle ordovician yijianfang formation in Tarim Basin. *J. Palaeogeogr.* 18 (06), 986–1001. (in Chinese with English abstract). doi:10.7605/gdxb.2016.06.075
- Gao, H. H., He, D. F., Tong, X. G., Wen, Z. X., and Wang, Z. M. (2017a). Tectonic-depositional environment and proto-type basin evolution of the cambrian in the Tarim Basin. *Geoscience* 31 (01), 102–118. (in Chinese with English abstract). doi:10.3969/j.issn.1000-8527.2017.01.009
- Gao, H. H., He, D. F., Tong, X. G., Wen, Z. X., Wang, Z. M., and Zhang, Y. Q. (2017b). Tectonic-depositional environment and proto-type basins evolution of the Tarim Basin in the late ordovician. *Earth Sci. Front.* 24 (05), 350–367. (in Chinese with English abstract). doi:10.13745/j.esf.yx.2016-10-3
- Gao, H. H. (2015). Tectonic-depositional setting and proto-type basin evolution of the Cambrian and Ordovician in Tarim area. *China University of Geosciences.* 52, 164.
- Gao, Z. Q., and Fan, T. L. (2015). Carbonate platform-margin architecture and its influence on Cambrian-Ordovician reef-shoal development, Tarim Basin, NW China. *Mar. Petroleum Geol.* 68, 291–306. doi:10.1016/j.marpetgeo.2015.08.033
- Gao, Z. Q., Fan, T. L., Yang, W. H., and Wang, X. (2012). Structure characteristics and evolution of the eopaleozoic carbonate platform in Tarim Basin. *J. Jilin Univ. (Earth Sci. Ed.)* 42 (03), 657–665. (in Chinese with English abstract). doi:10.13278/j.cnki.jjuese.2012.03.004
- Ge, R. F., Zhu, W. B., Wu, H. L., Zheng, B. H., Zhu, X. Q., and He, J. W. (2012). The paleozoic northern margin of the Tarim craton: Passive or active. *Lithos* 142, 1–15. doi:10.1016/j.lithos.2012.02.010
- He, B., Jiao, C., Xu, Z., Cai, Z., Zhang, J., Liu, S., et al. (2016). The paleotectonic and paleogeography reconstructions of the Tarim Basin and its adjacent areas (NW China) during the late Early and Middle Paleozoic. *Gondwana Res.* 30, 191–206. doi:10.1016/j.gr.2015.09.011
- He, B. Z., Jiao, C. L., Xu, Z. Q., Cai, Z. H., Liu, S. L., Zhang, J. X., et al. (2015). Distribution and migration of the phanerozoic palaeo-uplifts in the Tarim Basin, NW China. *Earth Sci. Front.* 22 (3), 277–289. (in Chinese with English abstract). doi:10.13745/j.esf.2015.03.024
- He, B. Z., Jiao, C. L., Xu, Z. Q., Liu, S. L., Cai, Z. H., Li, H. B., et al. (2013). Unconformity structural architecture and tectonic paleo-geographic environment: A case of the middle caledonion on the northern margin of Tibet Plateau and Tarim Basin. *Acta Petrol. Sin.* 29 (6), 2184–2198. (in Chinese with English abstract).
- He, D. F., Jia, C. Z., Li, D. S., Zhang, C. J., Meng, Q. R., and Shi, X. (2005). Formation and evolution of polycyclic superimposed Tarim Basin. *Oil & Gas Geol.* 26 (1), 64–77. (in Chinese with English abstract). doi:10.3321/j.issn:0253-9985.2005.01.010
- He, D. F., Li, D. S., and WangLiuChen, C. S. S. F. J. J. (2020). Status, thinking, and methodology of studying on the mobile tectono-palaeogeography. *J. Palaeogeogr.* 22 (01), 1–28. (in Chinese with English abstract). doi:10.7605/gdxb.2020.01.001
- He, D. F., Zhou, X. Y., Zhang, C. J., and Yang, X. F. (2007). Type and evolution of Ordovician proto-type basin in Tarim. *Chin. Sci. Bull.* 52, 126–135. (in Chinese). doi:10.3321/j.issn:0023-074x.2007.z1.015
- Hou, G. T., Santosh, M., Qian, X. L., Lister, G. S., and Li, J. H. (2008). Configuration of the Late Paleoproterozoic supercontinent Columbia: Insights from radiating mafic dyke swarms. *Gondwana Res.* 14 (3), 395–409. doi:10.1016/j.gr.2008.01.010
- Hou, M. C., Chen, A. Q., Ogg, J. G., Ogg, G. M., Huang, K. K., Xing, F. C., et al. (2019). China paleogeography: Current status and future challenges. *Earth-Science Rev.* 189, 177–193. doi:10.1016/j.earscirev.2018.04.004
- Hou, Z. S., Fan, J. X., Zhang, L. N., and Shen, S. Z. (2020). Construction method and comparison of global paleogeographic reconstruction models and associated knowledge discovery. *Geol. J. China Univ.* 26 (01), 86–99. (in Chinese with English abstract). doi:10.16108/i.issn1006-7493.2019105
- Huang, B. C., Piper, J. D. A., Sun, L. S., and Zhao, Q. (2019). New paleomagnetic results for Ordovician and Silurian rocks of the Tarim Block, Northwest China, and their paleogeographic implications. *Tectonophysics* 755, 91–108. doi:10.1016/j.tecto.2019.02.010
- Huang, B. C., Piper, J. D. A., and Zhu, R. X. (2009). Paleomagnetic constraints on neotectonic deformation in the Kashi depression of the Western Tarim Basin, NW China. *Int. J. Earth Sci.* 98 (6), 1469–1488. doi:10.1007/s00531-008-0401-5
- Huang, B. C., Yan, Y. G., Piper, J. D. A., Zhang, D. H., Yi, Z. Y., Yu, S., et al. (2018). Paleomagnetic constraints on the paleogeography of the east asian blocks during late paleozoic and early mesozoic times. *Earth-Science Rev.* 186, 8–36. doi:10.1016/j.earscirev.2018.02.004
- Huang, B. C., Zhou, T. X., and Zhu, R. X. (2008). Discussions on Phanerozoic evolution and formation of continental China, based on paleomagnetic studies. *Earth Sci. Front.* 15 (3), 348–359. (in Chinese with English abstract). doi:10.3321/j.issn:1005-2321.2008.03.031
- Huang, B. C., Zhu, R. X., Otofujii, Y., and Yang, Z. Y. (2000). Discussion on the Paleogeographic location of the main blocks in China in the early Paleozoic. *Chin. Sci. Bull.* (04), 337–345. (in Chinese). doi:10.3321/j.issn:0023-074X.2000.04.001
- Huang, H. M., Li, P. F., Hu, W. W., and Ling, J. Q. (2021). Early paleozoic collage of the Yili block, west tianshan: Constraints from U-Pb geochronology and Hf isotopes of clastic zircons. *Geotect. Metallogenia* 45 (04), 786–804. (in Chinese). doi:10.16539/j.ddgzyckx.2021.04.007
- Ji, H. L., He, Z. B., Qin, M. K., Wei, S. Y., Cao, J. H., and Yang, F. (2020). Sedimentary characteristics of lower cretaceous mangshigou formation in hegang sag, sanjiang basin, heilongjiang province. *Geol. Rev.* 66 (01), 52–68. (in Chinese).
- Jia, C. Z. (2004). *Plate tectonics and continental dynamics, Tarim Basin*. Beijing: Petroleum Industry Press, 1–202. (in Chinese).
- Jia, C. Z. (1997). *Structural characteristics and hydrocarbon in Tarim Basin*. China. Beijing: Petroleum Industry Press, 1–438. (in Chinese).
- Jia, J. H., Zhang, B. M., Zhu, S. H., Zhu, Y. C., and Li, Z. Y. (2006). Stratigraphy, sedimentary characteristics, and lithofacies palaeogeography of the Silurian in Tarim Basin. *J. Palaeogeogr.* 08 (03), 339–352. (in Chinese with English abstract).
- Jiang, T., Gao, J., Klemd, R., Qian, Q., Zhang, X., Xiong, X. M., et al. (2014). Paleozoic ophiolitic mélanges from the South Tianshan Orogen, NW China: Geological, geochemical and geochronological implications for the geodynamic setting. *Tectonophysics* 612–613, 106–127. doi:10.1016/j.tecto.2013.11.038
- Jiang, Z. X. (2010). *Sedimentology*. Beijing: Petroleum Industry Press, 1–507. (in Chinese).
- Johnson, M. R. W. (2002). Shortening budgets and the role of continental subduction during the India-Asia collision. *Earth-Science Rev.* 59, 101–123. doi:10.1016/S0012-8252(02)00071-5
- Kang, L., Liu, L., Cao, Y. T., Wang, C., Yang, W. Q., and Zhu, X. H. (2011). Geochemistry, zircon LA-ICP-MS U-Pb ages and Hf isotopes of Hongliugou moyite from north Altyn Tagh tectonic belt. *Geol. Bull. China* 30 (7), 1066–1076. (in Chinese with English abstract). doi:10.3969/j.issn.1671-2552.2011.07.009
- Laborde, A., Barrier, L., Simoes, M., Li, H., Coudroy, T., Van Der Woerd, J., et al. (2019). Cenozoic deformation of the Tarim Basin and surrounding ranges (xinjiang, China): A regional overview. *Earth-Science Rev.* 197, 102891. doi:10.1016/j.earscirev.2019.102891
- Li, J. H., and Jiang, H. F. (2013). *Global paleo-plate reconstruction, lithofacies Palaeogeography and paleoenvironment atlas*. Beijing: Geology Press, 1–127. (in Chinese).
- Li, J. H., Wang, H. H., Li, W. B., and Zhou, X. B. (2014). Discussion on global tectonics evolution from plate reconstruction in Phanerozoic. *Acta Pet. Sin.* 35 (2), 207–218. (in Chinese with English abstract). doi:10.7623/syxb201402001
- Li, J. H., Zhou, X. B., Li, W. B., Wang, H. H., Liu, Z. L., Zhang, H. T., et al. (2015). Preliminary reconstruction of tectonic paleogeography of Tarim Basin and its

- adjacent areas from Cambrian to Triassic, NW China. *Geol. Rev.* 61 (6), 1225–1234. (in Chinese).
- Li, J. Z., Zheng, M., Guo, Q. L., and Wang, S. J. (2019). *The fourth evaluation of hydrocarbon resources*. Beijing: Petroleum Industry Press, 1–385. (in Chinese).
- Li, Q. M., Wu, G. H., Pang, X. Q., Pan, W. Q., Luo, C. S., Wang, C. L., et al. (2010). Hydrocarbon accumulation conditions of ordovician carbonate in Tarim Basin. *Acta Geol. Sin. - Engl. Ed.* 84 (5), 1180–1194. doi:10.1111/j.1755-6724.2010.00289.x
- Li, S. B., Chen, B. L., Chen, Z. L., Hao, R. X., Zhou, Y. G., and Han, F. B. (2013). Petrogeochemical characteristics and tectonic setting of early Paleozoic intermediate-acid volcanic lava in Karadawan area, the northern margin of Altyn. *Geol. Rev.* 59 (3), 423–436. (in Chinese). doi:10.3969/j.issn.0371-5736.2013.03.003
- Li, S. Z., Zhao, S. J., LiuCao, X. H., Yu, S., Li, X. Y., Somerville, I., et al. (2017). Closure of the Proto-Tethys Ocean and early paleozoic amalgamation of microcontinental blocks in east asia. *Earth-Science Rev.* 186, 37–75. doi:10.1016/j.earscirev.2017.01.011
- Li, X. M., Xia, L. Q., Xia, Z. C., Xu, X. Y., Ma, Z. P., and Wang, L. S. (2006). Geochemical characteristics and petrogenesis of Neoproterozoic-Early Cambrian volcanic rocks in Tianshan area. *Acta Petrologica Mineralogica* (05), 412–422. (in Chinese with English abstract). doi:10.3969/j.issn.1000-6524.2006.05.005
- Li, X. P., Zhang, L. F., Wilde, S. A., Song, B., and Liu, X. M. (2010). Zircons from rodingite in the Western Tianshan serpentinite complex: Mineral chemistry and U-Pb ages define nature and timing of rodingitization. *Lithos* 118, 17–34. doi:10.1016/j.lithos.2010.03.009
- Li, Y. P., McWilliams, M., Sharps, R., Cox, A., Li, Y. A., Li, Q., et al. (1990). A Devonian paleomagnetic pole from red beds in the Tarim Block, China. *J. Geophys. Res.* 95 (B12), 19185–19198. doi:10.1029/JB095iB12p19185
- Li, Z. X., Bogdanova, S. V., Collins, A. S., Davidson, A., Waele, B. D., Ernst, R. E., et al. (2008). Assembly, configuration, and break-up history of Rodinia: A synthesis. *Precambrian Res.* 160 (1–2), 179–210. doi:10.1016/j.precamres.2007.04.021
- Lin, C. S., Li, S. T., Liu, J. Y., Qian, Y. X., Luo, H., Chen, J. Q., et al. (2011). Tectonic framework and paleogeographic evolution of the Tarim Basin during the Paleozoic major evolutionary stages. *Acta Petrol. Sin.* 27 (1), 210–218. (in Chinese with English abstract).
- Lin, C. S., Yang, H. J., Liu, J. Y., Cai, Z. Z., Peng, L., Yang, X. F., et al. (2008). Paleohigh geomorphology and paleogeographic framework and their controls on the formation and distribution of stratigraphic traps in the Tarim Basin. *Oil Gas Geol.* 29 (2), 189–197. (in Chinese with English abstract). doi:10.3321/j.issn:0253-9985.2008.02.006
- Lin, C. S., Yang, H. J., Liu, J. Y., Rui, Z. F., Cai, Z. Z., and Zhu, Y. F. (2012). Distribution and erosion of the Paleozoic tectonic unconformities in the Tarim Basin, Northwest China: Significance for the evolution of paleo-uplifts and tectonic geography during deformation. *J. Asian Earth Sci.* 46, 1–19. doi:10.1016/j.jseas.2011.10.004
- Liu, C. Y., Wang, J. Q., Zhao, X. C., Huang, L., Zhang, D. D., Zhao, J. F., et al. (2020). The proto-type basin and its nomenclature and research. *Petroleum Geol. Exp.* 42 (05), 720–727. (in Chinese with English abstract). doi:10.11781/sysydz202005720
- Liu, L., Liao, X. Y., Wang, Y. W., Wang, C., Santosh, M., Yang, M., et al. (2016). Early paleozoic tectonic evolution of the North Qinling orogenic belt in central China: Insights on continental deep subduction and multiphase exhumation. *Earth-Science Rev.* 159, 58–81. doi:10.1016/j.earscirev.2016.05.005
- Liu, L., Liao, X. Y., Zhang, C. L., Chen, D. L., Gong, X. K., and Kang, L. (2013). Multi-metamorphic timings of HP-UHP rocks in the North Qinling and their geological implications. *Acta Petrol. Sin.* 29, 1634–1656. (in Chinese with English abstract).
- Lou, Q. Q., Xiao, A. C., Zhong, N. C., and Wu, L. (2016). A method of proto-type restoration of large depressions with terrestrial sediments: A case study from the cenozoic Qaidam basin. *Acta Petrol. Sin.* 32 (03), 892–902. (in Chinese).
- Maruyama, S., Sawaki, Y., Ebisuzaki, T., Ikoma, M., Omori, S., and Komabayashi, T. (2014). Initiation of leaking Earth: An ultimate trigger of the Cambrian explosion. *Gondwana Res.* 25 (3), 910–944. doi:10.1016/j.jgr.2013.03.012
- Matte, P., Tapponnier, P., Arnaud, N., Bourjot, L., Avouac, J. P., Vidal, P., et al. (1996). Tectonics of western tibet, between the Tarim and the indus. *Elsevier* 142 (3–4), 311–330. doi:10.1016/0012-821x(96)00086-6
- Matthews, K. J., Maloney, K. T., Zahirovic, S., Williams, S. E., Seton, M., and Müller, R. D. (2016). Global plate boundary evolution and kinematics since the late Paleozoic. *Glob. Planet. Change* 146, 226–250. doi:10.1016/j.gloplacha.2016.10.002
- Meng, F. C., Zhang, J. X., Yu, S. X., and Chen, S. Y. (2010). Early paleozoic pillow basalt in hongliuquan, North Altyn, and its geotectonic significance. *Acta Geol. Sin.* 84 (7), 981–990. (in Chinese).
- Mou, D. L., Li, S. Z., Wang, Q., Li, X. Y., Wang, P. C., Yu, S. X., et al. (2018). The early paleozoic orocline in the southeastern Tarim Basin. *Acta Petrol. Sin.* 34 (12), 3739–3757. (in Chinese with English abstract).
- Nie, S. Y. (1991). Paleoclimatic and paleomagnetic constraints on the Paleozoic reconstructions of south China, north China, and Tarim. *Tectonophysics* 196 (3/4), 279–308. doi:10.1016/0040-1951(91)90327-o
- Rao, Y., Yu, S., Huang, X. W., and Chen, C. (2016). Hydrocarbon distribution regularity and main controlling factors analysis of Paleozoic reservoirs in Middle East. *Glob. Geol.* 35 (04), 1041–1051. (in Chinese with English abstract). doi:10.3969/j.issn.1004-5589.2016.04.014
- Shao, L. Y., Wang, X. T., Li, Y. N., and Liu, B. Q. (2019). Review on palaeogeographic reconstruction of deep-time source-to-sink systems. *J. Palaeogeogr.* 21 (01), 67–81. doi:10.7605/gdxb.2019.01.004
- Shen, P., Pan, H. D., Seitmuratova, E., Yuan, F., and Jakupova, S. (2016). A Cambrian intra-oceanic subduction system in the Bozshakol area, Kazakhstan. *Lithos* 224–225, 61–77. doi:10.1016/j.lithos.2015.02.025
- Sobel, E. R., and Araud, N. (1999). A possible middle paleozoic suture in the Altyn Tagh, NW China. *Tectonics* 18 (1), 64–74. doi:10.1029/1998tc900023
- Steinberger, B., Sutherland, R., and O'Connell, R. J. (2004). Prediction of Emperor-Hawaii seamount locations from a revised model of global plate motion and mantle flow. *Nature* 430, 167–173. doi:10.1038/nature02660
- Sun, L. S., and Huang, B. C. (2009). New paleomagnetic result for Ordovician rocks from the Tarim Block, Northwest China and its tectonic implications. *Chin. J. Geophys.* (07), 1836–1848. (in Chinese with English abstract). doi:10.3969/j.issn.0001-5733.2009.07.018
- Tian, J., Wang, Q. H., Yang, H. J., and Li, Y. (2021). Petroleum exploration history and enlightenment in Tarim Basin. *Xinjiang Pet. Geol.* 42 (03), 272–282. (in Chinese with English abstract). doi:10.7657/XJPG20210303
- Tian, L., Cui, H. F., Liu, J., Zhang, N. C., and Shi, X. X. (2018). Early-middle cambrian paleogeography and depositional evolution of Tarim Basin. *Oil Gas Geol.* 39 (05), 1011–1021. (in Chinese with English abstract). doi:10.11743/ogg20180515
- Tong, X. G., and He, D. F. (2021). *Principles and methods of hydrocarbon exploration*. Beijing: Petroleum Industry Press, 1–257.
- Torsvik, T. H., and Cocks, L. R. M. (2004). Earth geography from 400 to 250 Ma: A palaeomagnetic, faunal and facies review. *J. Geol. Soc.* 161, 555–572. doi:10.1144/0016-764903-098
- Torsvik, T. H., and Cocks, L. R. M. (2013). Gondwana from top to base in space and time. *Gondwana Res.* 24 (3–4), 999–1030. doi:10.1016/j.gr.2013.06.012
- Torsvik, T. H., and Cocks, L. R. M. (2019). The integration of palaeomagnetism, the geological record and mantle tomography in the location of ancient continents. *Geol. Mag.* 156, 242–260. doi:10.1017/s001675681700098x
- Torsvik, T. H., Steinberger, B., Ashwal, L. D., Doubrovine, P. V., and Trønnes, R. G. (2016). Earth evolution and dynamics-a tribute to Kevin Burke. *Can. J. Earth Sci.* 53, 1073–1087. doi:10.1139/cjes-2015-0228
- Van der Voo, R. (1993). *Paleomagnetism of atlantic, Tethys, and lapetus oceans*. Cambridge: Cambridge University Press, 1–411.
- Van der Voo, R. (1990). The reliability of paleomagnetic data. *Tectonophysics* 184, 1–9. doi:10.1016/0040-1951(90)90116-P
- Wang, B., Jahn, B. M., Shu, L. S., Li, K. S., Chung, S. L., and Liu, D. Y. (2012). Middle-late ordovician arc-type plutonism in the NW Chinese tianshan: Implication for the accretion of the Kazakhstan continent in central asia. *J. Asian Earth Sci.* 49, 40–53. doi:10.1016/j.jseas.2011.11.005
- Wang, B., Liu, H. S., Shu, L. S., Jahn, B. M., Chung, S. L., Zhai, Y. Z., et al. (2014a). Early Neoproterozoic crustal evolution in northern Yili Block: Insights from migmatite, orthogneiss, and leucogranite of the Wenquan metamorphic complex in the NW Chinese Tianshan. *Precambrian Res.* 242, 58–81. doi:10.1016/j.precamres.2013.12.006
- Wang, B., Shu, L. S., Faure, M., Jahn, B. M., Cluzel, D., Charvet, J., et al. (2011). Paleozoic tectonics of the southern Chinese Tianshan: Insights from structural, chronological and geochemical studies of the Heiyingshan ophiolitic mélange (NW China). *Tectonophysics* 497, 85–104. doi:10.1016/j.tecto.2010.11.004
- Wang, B., Shu, L. S., Liu, H. S., Gong, H. J., Ma, Y. Z., Mu, L. X., et al. (2014b). First evidence for ca. 780 Ma intra-plate magmatism and its implications for Neoproterozoic rifting of the North Yili Block and tectonic origin of the continental blocks in SW of Central Asia. *Precambrian Res.* 254, 258–272. doi:10.1016/j.precamres.2014.09.005
- Wang, C., Luo, J. H., Che, Z. C., Liu, L., and Zhang, J. Y. (2009). Geochemical characteristics and zircon LA-ICP-MS dating of the oxidaban granite in xinjiang: Implications for the subduction process of the paleozoic Ocean in southwestern tianshan. *Acta Geol. Sin.* 83 (2), 272–283. (in Chinese). doi:10.3321/j.issn:0001-5717.2009.02.012
- Wang, C. S., and Lin, C. S. (2021). Development status and trend of sedimentology in China in recent ten years. *Bull. Mineralogy, Petrology Geochem.* 40 (06), 1217. (in Chinese with English abstract). doi:10.19658/j.issn.1007-2802.2021.40.096
- Wang, C. S., Zheng, H. R., Ran, B., Liu, B. P., Li, X. H., Li, Y. L., et al. (2010). Practice and reflection on reconstruction of active paleogeography: A case study in the qinghai-tibet Tethys. *Acta Sedimentologica Sin.* (05), 849–860. (in Chinese). doi:10.14027/j.cnki.cjxb.2010.05.002
- Wang, P., Zhao, G., Han, Y., Liu, Q., Yao, J., and Yu, S. (2021). Position of the Tarim craton in Gondwana: Constraints from neoproterozoic to early paleozoic strata in south Tarim, NW China. *Tectonophysics* 803, 228741. doi:10.1016/j.tecto.2021.228741
- Wang, T., Zheng, M. L., Ren, H. J., Li, T., Wu, H. S., Wang, X. L., et al. (2021). New understandings of stratigraphic division and correlation of Jiamuhe Formation and natural gas exploration target in Mahu Sag and its periphery, Junggar Basin. *China Pet. Explor.* 26 (04), 99–112. (in Chinese with English abstract). doi:10.3969/j.issn.1672-7703.2021.04.008
- Wen, B., Evans, D. A. D., and Li, Y. X. (2017). Neoproterozoic paleogeography of the Tarim Block: An extended or alternative “missing-link” model for Rodinia? *Earth Planet. Sci. Lett.* 458, 92–106. doi:10.1016/j.epsl.2016.10.030
- Wu, C. L., Yang, J. S., Yao, S. Z., Zeng, L. S., Chen, Y. S., Li, H. B., et al. (2005). Characteristics of the granitoid complex and its zircon SHRIMP dating at the south margin

- of the Bashikaogong Basin, North Altyn, NW China. *Acta Petrol. Sin.* 21 (3), 846–858. (in Chinese with English abstract). doi:10.3321/j.issn:1000-0569.2005.03.024
- Wu, C. L., Yao, S. Z., Zeng, L. S., Yang, J. S., Wooden, J. L., Chen, Y. S., et al. (2007). Characteristics and SHRIMP U-Pb zircon dating of the Bashikaogong-Smilbrak granitic complex in the northern Altyn. *Sci. China (Series D Earth Sci.* 37 (1), 10–26. (in Chinese).
- Wu, G. H., Chen, X., Ma, B. S., Chen, Y. Q., Tian, W. Z., Huang, S. Y., et al. (2021). The tectonic environments of the late neoproterozoic-early paleozoic and its tectono-sedimentary response in the Tarim Basin. *Acta Petrol. Sin.* 37 (08), 2431–2441. (in Chinese with English abstract). doi:10.18654/1000-0569/2021.08.11
- Wu, G. H., Deng, W., Huang, S. Y., Zheng, D. M., and Pan, W. Q. (2020). Tectonic-paleogeographic evolution of the Tarim Basin. *Chin. J. Geol.* 55 (02), 305–321. (in Chinese). doi:10.12017/dzcx.2020.020
- Wu, G. H., Pang, X. Q., Li, Q. M., and Yang, H. J. (2016). *Structural characteristics in intracratonic carbonate rocks and its implication for oil/gas accumulation: A case study in the Tarim Basin*. China. Beijing: Science Press, 1–344. (in Chinese).
- Wu, L., Guan, S. W., Zhang, S. C., Yang, H. J., Jin, J. Q., Zhang, X. D., et al. (2018). Neoproterozoic stratigraphic framework of the Tarim Craton in NW China: Implications for rift evolution. *J. Asian Earth Sci.* 158, 240–252. doi:10.1016/j.jseas.2018.03.003
- Xiao, W. J., Huang, B. C., Han, C. M., Sun, S., and Li, J. L. (2010). A review of the Western part of the altids: A key to understanding the architecture of accretionary orogens. *Gondwana Res.* 18 (2), 253–273. doi:10.1016/j.gr.2010.01.007
- Xiao, W. J., Windley, B. F., Yuan, C., Sun, M., Han, C. M., Lin, S. F., et al. (2009). Paleozoic multiple subduction-accretion processes of the Southern Altids. *Am. J. Sci.* 309, 221–270. doi:10.2475/03.2009.02
- Xiao, X. C., Wang, J., Su, L., and Song, S. G. (2003). A further discussion of the Kudi ophiolite, west Kunlun, and its tectonic significance. *Geol. Bull. China* 22 (10), 745–750. (in Chinese). doi:10.3969/j.issn.1671-2552.2003.10.001
- Xiu, Q. Y., Yu, H. F., Liu, Y. S., Lu, S. N., Mao, D. B., Li, H. M., et al. (2007). Characteristics and SHRIMP U-Pb zircon dating of the pillow basalt in the northern Altyn. *Acta Geol. Sin.* 81 (6), 787–794. (in Chinese). doi:10.3321/j.issn:0001-5717.2007.06.006
- Xu, B., Xiao, S. H., Zou, H. B., Chen, Y., Li, Z. X., Song, B., et al. (2008). SHRIMP zircon U-Pb age constraints on Neoproterozoic Quruqtagh diamicites in NW China. *Precambrian Res.* 168 (3–4), 247–258. doi:10.1016/j.precamres.2008.10.008
- Xu, Z. Q., Li, S. T., Zhang, J. X., Yang, J. S., He, B. Z., Li, H. B., et al. (2011). Paleo-Asian and Tethyan tectonic systems with docking the Tarim block. *Acta Petrol. Sin.* 27 (1), 1–22. (in Chinese with English abstract).
- Xu, Z. Q., Yang, J. S., Zhang, J. X., Jiang, M., Li, H. B., and Cui, J. W. (1999). Comparison of tectonic units on both sides of Altyn fault and lithospheric shear mechanism. *Acta Geol. Sin.* 73 (3), 193–205. (in Chinese). doi:10.3321/j.issn:0001-5717.1999.03.001
- Yang, J. S., Shi, R. D., Wu, C. L., Su, D. C., Chen, S. Y., Wang, X. B., et al. (2008). Petrology and SHRIMP age of the Hongliugou ophiolite at Milan, north Altyn, at the northern margin of the Tibetan plateau. *Acta Petrol. Sin.* 24 (7), 1567–1584. (in Chinese with English abstract).
- Yang, Z. J., Ma, D. H., Wang, Z. X., and Xiao, W. F. (2012). SHRIMP U-Pb zircon dating of gabbro from the Binggou ophiolite mélange in the northern Altyn, and geological implication. *Acta Petrol. Sin.* 28 (7), 2269–2276. (in Chinese with English abstract).
- Yang, Z. Y., Sun, Z. M., Yang, T. S., and Pei, J. L. (2004). A long connection (750–380 Ma) between south China and Australia: Paleomagnetic constraints. *Earth Planet. Sci. Lett.* 220, 423–434. doi:10.1016/S0012-821X(04)00053-6
- Yu, H. B., Qi, J. F., Yang, X. Z., Sun, T., Liu, Q. X., and Cao, S. J. (2016). Analysis of mesozoic proto-type basin in kuga depression, Tarim Basin. *Xinjiang Pet. Geol.* 37 (06), 644–653+666. (in Chinese with English abstract). doi:10.7657/XJPG20160604
- Yun, J. B., Jin, Z. J., and Xie, G. J. (2014). Distribution of major hydrocarbon source rocks in the lower paleozoic, Tarim Basin. *Oil Gas Geol.* 35 (06), 827–838. (in Chinese with English abstract). doi:10.11743/ogg201406010
- Zhang, C. L., Lu, S. N., Yu, H. F., and Ye, H. M. (2007). Tectonic evolution of western orogenic belt: Evidences from zircon SHRIMP and LA-ICP-MS U-Pb ages. *Sci. China (Series D)* 50, 1–12.
- Zhang, C. L., Yu, H. F., Shen, J. L., Dong, J. G., Yie, H. M., and Guo, K. Y. (2004). Zircon SHRIMP age determination of the giant-crystal gabbro and basalt in K(u)da, west Kunlun: Dismembering of the Kudi ophiolite. *Geol. Rev.* 50 (6), 639–643. doi:10.16509/j.georeview.2004.06.013
- Zhang, C. L., Zou, H. Bo., YeTao, X., and ChenYan, X. (2019). Tectonic evolution of the West Kunlun orogenic belt along the northern margin of the Tibetan plateau: Implications for the assembly of the Tarim terrane to Gondwana. *Geosci. Front.* 10 (03), 973–988. doi:10.1016/j.gsf.2018.05.006
- Zhang, G. Y., Liu, W., Zhang, L., Yu, B. S., Li, H. H., Zhang, B. M., et al. (2015). Cambrian-Ordovician prototypic basin, paleogeography, and petroleum of Tarim Craton. *Earth Sci. Front.* 22 (3), 269–276. (in Chinese with English abstract). doi:10.13745/j.esf.2015.03.023
- Zhang, G. Y., Tong, X. G., Xin, R. C., Wen, Z. X., Ma, F., Huang, T. F., et al. (2019a). Evolution of lithofacies and paleogeography and hydrocarbon distribution worldwide (I). *Petroleum Explor. Dev.* 46 (04), 664–686. doi:10.1016/S1876-3804(19)60225-9
- Zhang, L. N., Fan, J. X., and Chen, Q. (2019b). Deep-time paleogeographic reconstruction based on database: Taking the South China T. Approximatus biozone (early ordovician) as an example. *Acta Geol. Sin. Engl. Ed.* 93 (S1), 76–79. doi:10.1111/1755-6724.14251
- Zhang, X. B., Zhang, S. N., Zhao, X. K., He, J. J., Li, K., Dai, H. S., et al. (2007). Calculation of denudation thickness of superimposed basin by seism stratigraphic comprehensive method: A case study from the akeule uplift in Tarim Basin. *Xinjiang Pet. Geol.* (03), 366–368. (in Chinese). doi:10.3969/j.issn.1001-3873.2007.03.030
- Zhang, Y., Niu, Y. L., Hu, Y., Liu, J. J., Ye, L., Kong, J. J., et al. (2016). The syncollisional granitoid magmatism and continental crust growth in the West Kunlun Orogen, China-evidence from geochronology and geochemistry of the Arkarz pluton. *Lithos* 245, 191–204. doi:10.1016/j.lithos.2015.05.007
- Zhang, Z. C., Guo, Z. J., and Song, B. (2009). SHRIMP zircon dating of gabbro from the ophiolite mélange in the northern Altyn Tagh and its geological implications. *Acta Petrol. Sin.* 25 (3), 568–576. (in Chinese with English abstract).
- Zhao, G. C., Wang, Y. J., Huang, B. C., Dong, Y. P., Li, S. Z., Zhang, G. W., et al. (2018). Geological reconstructions of the east asian blocks: From the breakup of Rodinia to the assembly of pangea. *Earth-Science Rev.* 186, 262–286. doi:10.1016/j.earscirev.2018.10.003
- Zheng, M. L., Wang, Y., Jin, Z. J., Li, J. Z., Zhang, Z. P., Jiang, H. S., et al. (2014). Superimposition, evolution, and petroleum accumulation of Tarim Basin. *Oil Gas Geol.* 35 (06), 925–934. (in Chinese with English abstract). doi:10.11743/ogg20140619
- Zheng, X. J., Du, Y. S., Zhu, X. M., Liu, Z. J., Hu, B., Wu, S. H., et al. (2021). The main progresses of Chinese paleogeography in the past decade. *Bull. Mineralogy, Petrology Geochem.* 40 (01), 94–114+4. (in Chinese with English abstract). doi:10.19658/j.issn.1007-2802.2020.39.089
- Zhou, D. W., Su, L., Jian, P., Wang, R. S., Liu, X. M., Lu, G. X., et al. (2004). SHRIMP zircon U-Pb age and tectonic significance of high-pressure granulite in Yushugou ophiolite terrane, South Tianshan. *Acta Petrol. Sin.* 49 (14), 1411–1413. (in Chinese). doi:10.3321/j.issn:0023-074X.2004.14.013
- Zhou, K. K., Mou, C. L., Ge, X. Y., Liang, W., Chen, X. W., Wang, Q. Y., et al. (2017). The reflection of the new lithofacies palaeogeographic mapping on the major geological problems in south China: The evolution of "the South China unified plate" in the late early paleozoic. *Acta Sedimentol. Sin.* 35 (03), 449–459. (in Chinese). doi:10.14027/j.cnki.cjxb.2017.03.003
- Zhu, R. X., Yang, Z. Y., Wu, H. N., Ma, X. H., Huang, B. C., Meng, Z. F., et al. (1998). Paleomagnetic constrains on the tectonic history of the major blocks of China since the Phanerozoic. *Sci. China (Series D Earth Sci.* 41, 1–19.